Surface Pressure and Precipitation Life Cycle Characteristics of PRE-STORM Mesoscale Convective Systems

SCOT M. LOEHRER* AND RICHARD H. JOHNSON

Department of Atmospheric Science, Colorado State University, Fort Collins, Colorado

(Manuscript received 3 March 1994, in final form 3 August 1994)

ABSTRACT

Extensive observations of the May–June 1985 Oklahoma–Kansas Preliminary Regional Experiment for STORM-Central (OK PRE-STORM) are used to examine the life cycle characteristics of 16 mesoscale convective systems (MCSs). The primary focus is on the surface pressure, flow, and precipitation structures of the MCSs.

It is found that despite the wide variety of initial precipitation structures of the MCSs, repeatable patterns developed in 75% of the cases during their mature-to-dissipating stages. The precipitation structure at this later stage of the life cycle can be described as asymmetric, following the definition of Houze et al. Due to the variety of directions of movement, the systems are examined in a motion-relative quadrant perspective. One axis is along the direction of system motion and the other perpendicular to it, crossing at the center of the convective line. The asymmetry is characterized by 1) a leading convective line containing relatively weak cells on the northern end and a trailing stratiform region in the left-rear quadrant (although in three of the cases there was also leading stratiform rain in the left-front quadrant) and 2) a leading convective line with progressively more intense cells on the southern end and a distinct lack of trailing stratiform precipitation in the right-rear quadrant. All MCSs possessed a surface presquall mesolow, mesohigh, and wake low during some period in their life cycles. Notably, the asymmetric pattern developed at the stage of the maximum pressure gradient between the mesohigh and the wake low. At this stage, the mesohigh often extended well into the stratiform region and the wake low was at its deepest point. Very intense pressure gradients were observed, averaging 2 mb (10 km)$^{-1}$, but ranging up to 5 mb (10 km)$^{-1}$. The flow in several cases passed through the wake low at or near severe limits (25 m s^{-1}).

A major finding of this paper is that while the symmetric and asymmetric MCS classification of Houze et al. is confirmed, these patterns characterize the precipitation structures at different stages of the life cycle rather than representing specific types of MCSs. The symmetric structure, if present, occurs during the earlier stages of development. The asymmetric structure predominates during the latter stages of the life cycle. There were four general paths taken by the MCSs from their widely varying initial structures to the asymmetrical structure. These paths are referred to as disorganized, back-building, linear, and intersecting convective bands. Some cases exhibited combinations of these paths. Conceptual models of the symmetric and asymmetric patterns, along with their corresponding surface pressure fields, are presented.

1. Introduction

Given the wide variety of types and scales of mesoscale convective organization, there have been many attempts to classify such structures. One approach has been to choose a particular, important defining characteristic and examine the subset of mesoscale convective systems (MCSs) that exhibit that characteristic. Some examples of such MCS subsets are mesoscale convective complexes (MCCs), squall lines, bow echoes, and derechos. MCCs are MCSs that have a large, long-lived, quasi-circular appearance in infrared satellite data (Maddox 1980). Squall lines, in a general sense, are propagating convective bands. Bow echoes are squall lines that have distinct curved convective lines on radar (Fujita 1978). Derechos are particularly severe bow echoes defined by their long-lived, widespread wind damage reports (Johns and Hirt 1987). The studies examining a large number of MCCs (Maddox 1983; Cotton et al. 1989) and derechos (Johns and Hirt 1987; Johns et al. 1990) have tended to focus on the large-scale environment accompanying such systems rather than their precipitation structure. Studies of MCC precipitation have generally focused on system-wide total precipitation characteristics (Kane et al. 1987; McAnelly and Cotton 1989) rather than radar reflectivity structures.

Instead of examining MCS subsets, another way to classify MCSs is to examine all MCSs for repeatable

* Current affiliation: Office of Field Project Support, University Corporation for Atmospheric Research, Boulder, Colorado.

Corresponding author address: Scot M. Loehrer, UCAR/OFPS, P.O. Box 3000, Boulder, CO 80307-3000.

structures. Few studies have been able to examine a large number of MCSs of all types to obtain documentation of their precipitation, surface pressure, and/or life cycle characteristics. Bluestein and Jain (1985) examined the formation characteristics of 40 severe squall lines in Oklahoma. They found four basic patterns of squall-line formation (see their Fig. 1) that they termed "broken line" (35%), "back building" (33%), "broken areal" (20%), and "embedded areal" (13%). Bluestein et al. (1987) conducted an identical study of 45 nonsevere convective lines. They found similar proportions of "broken line" (36%) and "embedded areal" (2%) but significantly less "back building" (13%) and more "broken areal" (49%) squall lines. Due to their focus on the formation characteristics, the latter portions of the life cycle were neglected.

Houze et al. (1990) conducted a similar study that focused more on the stage of maximum radar echo coverage within 200 km of the National Severe Storms Laboratory (NSSL)–Norman WSR-57 radar. The maximum radar echo coverage tends to occur within the mature stage of the MCS life cycle (Houze et al. 1989). They examined 63 MCSs that occurred over six years in Oklahoma. Two-thirds of the MCSs had a precipitation structure, termed classifiable, that consisted of a leading convective line and a trailing stratiform precipitation region. Within the classifiable MCSs, two prominent patterns were identified: *symmetric* and *asymmetric*. The symmetric MCS (Fig. 1a) has an arc-shaped, northeast–southwest-oriented leading convective line with the most intense convection present in the central portion of the line. Also, there is a region of enhanced stratiform precipitation located in approximately equal proportions in both the left-rear (LR) and right-rear (RR) quadrants of the system (Fig. 1c). The quadrant designations in Fig. 1c have been introduced to allow all of the systems in our study to be viewed in the same motion-relative context. That is, since there was a wide range of system movement during PRE-STORM, a coordinate system has been constructed that has axes parallel and perpendicular to the storm motion vector, crossing at the center of the convective line.

The asymmetric MCS (Fig. 1b) is similar but has a tendency for the most intense convection to be located at the southern end of the line. Also, the stratiform precipitation is displaced more to the LR quadrant and very little is within the RR quadrant of the system. Of the classifiable MCSs, they found that 26% were symmetric, 35% were asymmetric, and 38% were an intermediate combination of the two. Due to their use of only the single NSSL–Norman WSR-57 radar, they were only able to examine the MCSs at the stages they were in as they passed within 200 km of the radar site.

In another study, Blanchard (1990) attempted to classify the life cycle characteristics of MCS precipitation structure using the six-radar network of the May–June 1985 Oklahoma–Kansas Preliminary Regional Experiment for STORM-Central (OK PRE-STORM) field program (Cunning 1986). The study examined 25 MCSs and found three basic convective life cycle patterns (see his Fig. 2): "linear" (68%), "chaotic" (24%), and "occluding" (8%). Doswell (1991) questioned the use of the terms "occluding" and "chaotic" as they seem to give connotations to the radar structures the author may not have intended. Also, the term "linear" tended to be used in a rather

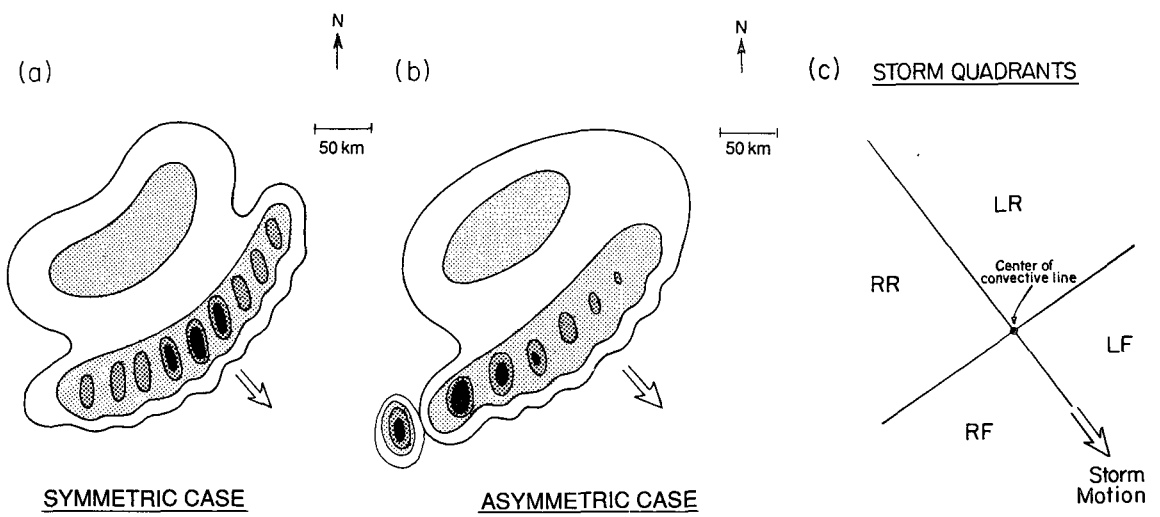

FIG. 1. Schematic of (a) symmetric and (b) asymmetric leading line–trailing stratiform mesoscale precipitation system organization (from Houze et al. 1990). Large vector indicates direction of system motion. Levels of shading denote increasing radar reflectivity, with most intense values corresponding to convective cell cores. A sample of the storm-motion-relative quadrants is shown in (c). The large arrow represents storm motion and the quadrants are defined as left rear (LR), right rear (RR), left front (LF), and right front (RF).

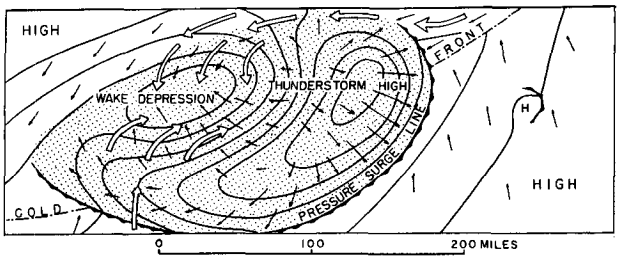

FIG. 2. Conceptual model of surface pressure field during the mature stage of a squall line. Small arrows indicate surface wind; large arrows relative flow into the wake. Stippling indicates extent of precipitation-cooled air (from Fujita 1955).

all-inclusive nature and the complete life cycle was not fully taken into account. In particular, Doswell notes one case that Blanchard placed into the linear category that later in its life cycle came to more closely resemble the occluding structure. So the question of the precipitation life cycle of MCSs is still largely unresolved.

Past studies of MCSs have indicated a close relationship between their precipitation structures and surface pressure patterns (Fujita 1955, 1963; Pedgley 1962; Johnson and Hamilton 1988). For example, in many squall lines a mesolow (the presquall mesolow) (Hoxit et al. 1976) is ahead of the leading convective line, a mesohigh is positioned just behind the leading convective line, and a mesolow (the *wake low*) is near the back edge of the trailing stratiform precipitation region. It is, therefore, instructive to investigate the life cycles of all features together. However, such studies have been limited to a small number of cases due to the need for simultaneous dense surface pressure observations and radar data over an extensive area. PRE-STORM represents one of the few opportunities for studying these features concurrently (Johnson and Hamilton 1988; Johnson et al. 1989; Stumpf et al. 1991).

Conceptual models that have been developed of the precipitation and surface pressure fields of MCSs have focused on the mature stage and have shown the existence of two basic types, with the precipitation patterns resembling either the symmetric (Fig. 1a) or asymmetric (Fig. 1b) MCSs of Houze et al. (1990). A structure fitting into the symmetric classification was first presented schematically by Fujita (1955) based on his examination of several MCSs that occurred over the central United States (Fig. 2). The schematic was constructed without radar data, so separation of the precipitation field into convective and stratiform components was not possible. The precipitation patterns were reconstructed using the surface station reports. The surface pressure pattern consists of two major features, a mesohigh ("thunderstorm high") and a wake low ("wake depression"). The mesohigh is positioned along the leading portion of the MCS in the region of rain-cooled downdrafts (Fujita 1959) and the wake low along the back-central portion of the MCS ahead of the rain termination line. There are two regions of intense pressure gradients: one is at the leading edge indicative of cool downdraft air, the gust front ("pressure surge line"); the other is between the mesohigh and wake low. The flow field shows strong outflow accelerating through the mesohigh, a diffluent zone between the mesohigh and wake low, and a confluent zone along the axis of the wake low. The flow through the wake low region is shown with about the same speed as the flow in the surrounding environment and is much weaker than along the leading gust front. Fujita (1963) expanded on this mature stage conceptual model by developing the life cycle characteristics of MCSs (see his Fig. 43). Due to the lack of radar data, only the surface pressure life cycle was considered. He shows a nearly symmetric structure during the entire life cycle, with the maximum pressure gradient between the wake low and mesohigh found during the mature-to-dissipating stage.

The conceptual model of Fujita (1955) for a symmetric MCS was adjusted by Johnson and Hamilton (1988) based on their study of the 10–11 June 1985 PRE-STORM MCS (Fig. 3). First, they found the existence of a presquall mesolow. Also, with the addition of radar data they show three primary features in the reflectivity fields: a leading convective line, followed by a transition zone (a region of minimum reflectivity), and then an enhanced region of stratiform precipitation (Chong et al. 1987; Smull and Houze 1987; Rutledge et al. 1988), with a wake low positioned along the back edge of the precipitation (Williams 1953, 1954; Pedgley 1962; Zipser 1977). Finally, they found the confluent zone, which Fujita placed along the wake-low axis, to be displaced to the rear of the wake-low axis as a

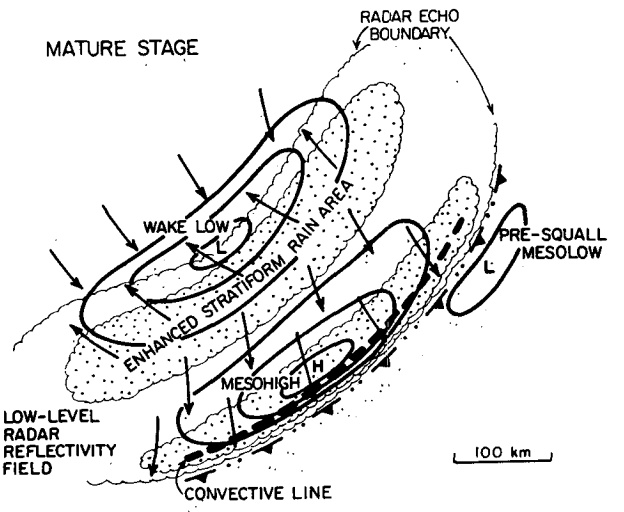

FIG. 3. Conceptual model of surface pressure, wind field, and precipitation during the mature stage of a squall line with a trailing stratiform rain region. Arrows indicate ground-relative surface winds (from Johnson and Hamilton 1988).

result of the system propagation (Garratt and Physick 1983; Vescio and Johnson 1992). The flow speed in the wake-low region is depicted as being approximately the same as along the leading gust front.

A conceptual model for an asymmetric MCS was presented by Pedgley (1962) based on a few MCSs that occurred in England on 28 August 1958 (Fig. 4). In many respects the schematic is similar to Fujita (1955), but there are important differences. Pedgley shows a displacement of the stratiform precipitation to the northwestern end of the MCS (LR quadrant). The wake low is also displaced to the rear of the far northwestern portion of the convective line along the back edge of the precipitation. Viewed from a storm-motion-relative perspective it very much resembles the asymmetric MCS of Houze et al. (1990).

Recent modeling work (Weisman 1993; Skamarock et al. 1994) has begun to address the question of symmetry/asymmetry of squall lines. A three-dimensional simulation of a squall line of finite extent indicates the existence of important line-end effects. In particular, a cyclonic circulation develops at the northern end and an anticyclonic circulation at the southern end. Without Coriolis effects, these two circulations are of approximately equal intensity and the MCS retains its symmetry (Weisman 1993). When the Coriolis effects are included in the simulation, the northern cyclonic circulation is enhanced, while the southern anticyclonic

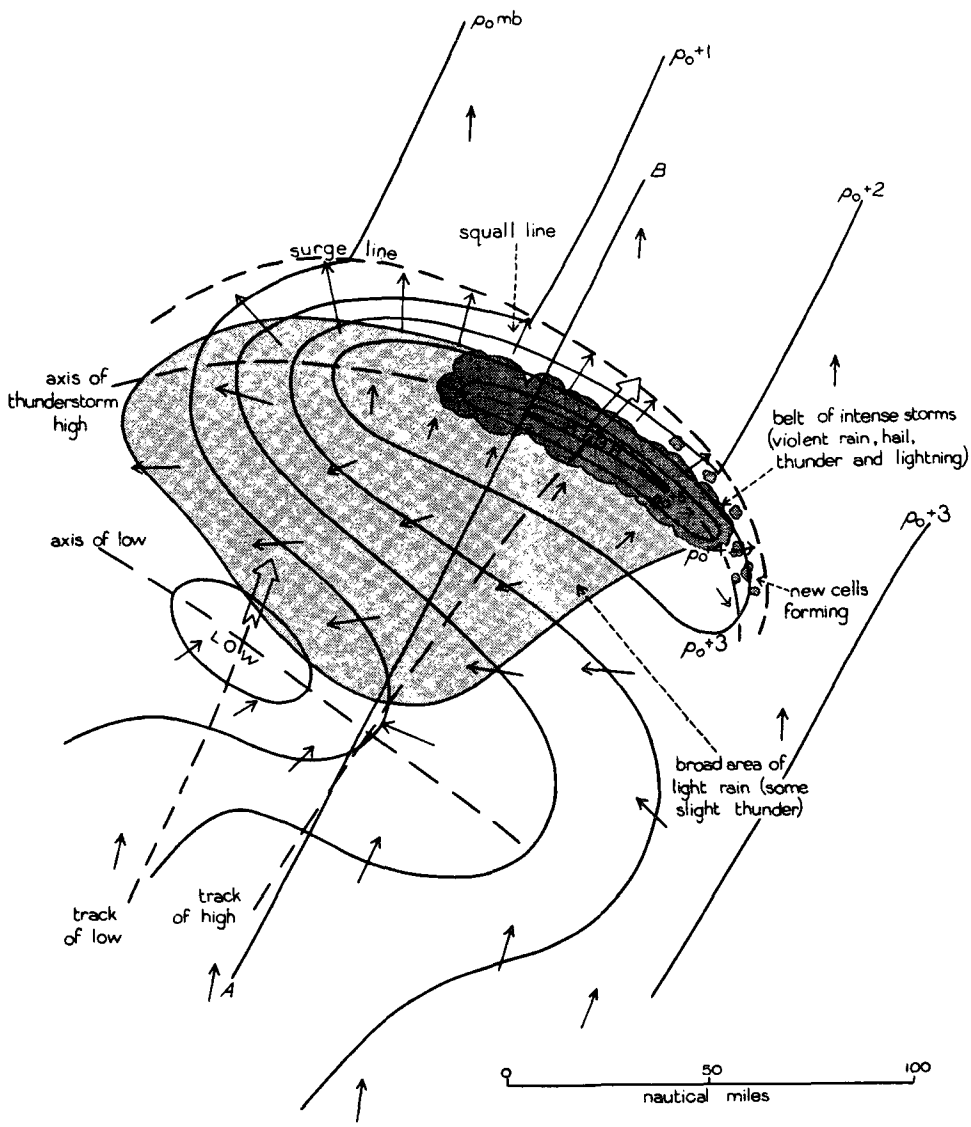

FIG. 4. Conceptual model of surface pressure, wind field, and precipitation during the mature stage of a squall line with a trailing stratiform rain region. Arrows indicate surface winds (from Pedgley 1962).

circulation is diminished (Skamarock et al. 1994). In these Coriolis simulations an initially symmetric MCS develops into an asymmetric MCS at later portions of its life cycle. An important question is whether there is a tendency for observed MCSs to develop such an asymmetry.

This paper addresses this question by examining the majority of the MCSs observed during the PRE-STORM field program. Here we focus on observations of the life cycle characteristics of the surface pressure, flow, and precipitation structures.

The paper begins with a summary of the data and analysis procedures in section 2. The case selection procedure is briefly discussed in section 3. Section 4 covers the pre-MCS large-scale conditions. The diurnal variation of MCS stages is discussed in section 5. In section 6 the surface pressure and precipitation structures as well as the life cycle of MCSs are covered, including a brief discussion of the stability and thermodynamic characteristics. The final section includes a discussion of a revised conceptual model and a summary.

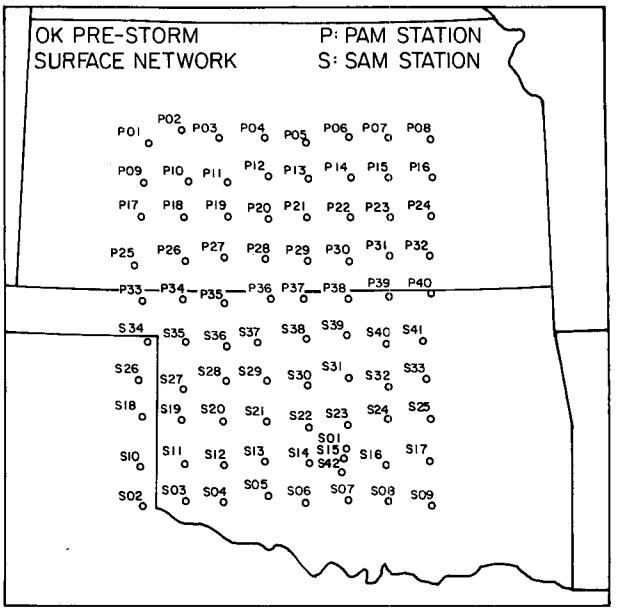

FIG. 5. The PRE-STORM surface mesonetwork.

2. Data and analysis procedures

a. Surface data

The PRE-STORM surface mesonetwork was composed of 84 automated stations. The northern portion of the network consisted of 40 National Center for Atmospheric Research (NCAR) Portable Automated Mesonetwork II (PAM) sites. In the southern portion, 40 NSSL Surface Automated Mesonetwork (SAM) stations were used. Additionally, two PAM sites were collocated with two SAM sites. The stations were located in an 8×10 rectangular array with an approximate spacing of 50 km (Fig. 5). Each of the stations provided 5-min averages of the dry- and wet-bulb temperatures, station pressure, wind direction, and wind speed. Also, the accumulated rainfall was measured at 5-min intervals and the maximum wind gust in the 5-min period was recorded.

Station pressures were adjusted hydrostatically to 480 m, the average elevation for all stations in the network, by approximating the mean virtual temperature of the column from the station elevation to 480 m by the surface virtual temperature. Atmospheric tidal effects were removed using the procedure described in Stumpf et al. (1991).

An adjustment was also made to remove the pressure errors resulting from individual station biases. The methodology used here is generally the same used in Stumpf et al. (1991) but it was applied over the entire PRE-STORM period. The procedure consisted of an intercomparison of the surrounding, well-calibrated National Weather Service stations with the PRE-STORM mesonet sites (Fujita 1963, Johnson and Toth 1986). The intercomparisons were done at times of generally "undisturbed" conditions, with weak pressure gradients and little convection, at times close to the entrance of the systems into the mesonet. Ten such time periods were chosen. The number of time periods was limited due to short intervals between several cases, leaving no extended period of inactivity. The biases were mostly in the range of -2 to $+2$ mb. The importance of applying this procedure for the 10 separate time periods is seen by the fact that the biases for each station varied by approximately 1 mb over the PRE-STORM period. Most variations were in the range of 0.5–1.5 mb, but five stations had variations of over 2 mb. Station PAM 32 (Fig. 5) had an extreme bias variation of 5.37 mb and had drastic shifts in its biases from case to case. The causes for such shifts are not known. Although the bias variations for the PAM and SAM sites were similar, the SAM sites had more problems with outages and bad surface pressure reports. Also, the PAM sites showed no overall positive or negative bias. The SAM sites, however, had 86% negative biases. The complete set of the applied bias corrections can be found in Loehrer (1992).

The pressure analyses were produced through the use of a Barnes-type scheme (Barnes 1964, 1973). Due to the presence of very strong pressure gradients in many cases, a time-to-space transformation procedure (Fujita 1963) was applied to the 5-min data to more accurately reflect these strong gradients. To do an analysis for some specific time, the 5-min data from 15 min before to 15 min after the specific time were used. The assumption was made that the systems were relatively steady state over the half-hour period. To properly position each of these data points, the velocity of each

TABLE 1. Cases examined and their calculated velocities. The 21 May 1985 convective line was not within the mesonet. Also indicated is the existence of a mesovortex in either the total or perturbation flow within the PRE-STORM region. Cases listed as unknown had inadequate upper-air data. Dates are taken from the time of maximum wake-low extent.

Case number	Date	Speed ($m\ s^{-1}$)	Direction (deg)	Mesovortex
1	7 May	19.2	287	yes
2	13 May (northern)	20.0	213	unknown
3	13 May (southern)	16.2	275	unknown
4	21 May	—	—	yes
5	27 May	17.5	280	unknown
6	28 May	18.3	300	yes
7	29 May	16.2	330	unknown
8	3 June	18.5	260	no
9	3–4 June	18.6	250	yes, weak
10	4 June	19.0	246	yes, weak
11	9 June	10.1	290	yes
12	11 June	15.6	308	yes, weak
13	15 June	12.1	338	no
14	22 June	9.8	340	yes
15	24 June	10.0	350	yes
16	27 June	8.6	316	no

system was calculated from the average velocity of the leading edge of the convective line over the lifetime of the system within the PRE-STORM area (Table 1). In cases without a well-defined leading convective line, the system velocity was calculated using an average velocity of the leading portion of the system. The data points were then placed in a string along either side of the station. This was done every 15 min throughout the lifetime of the system within the PRE-STORM region. In some cases, the trailing stratiform region moved somewhat more slowly than the leading convective line. Since the above procedure uses the speed of the convective line, the resulting pressure gradient between the mesohigh and wake low may be actually somewhat underestimated in those cases.

b. Radar and satellite data

Base-scan reflectivity data from the National Weather Service (NWS) WSR-57 radars at Amarillo, Texas; Oklahoma City and Norman, Oklahoma; Wichita and Garden City, Kansas; and Monett, Missouri were used. The low-level base scan (0.5° elevation angle) reflectivity data were used to construct the composite radar images, which consist of the digitized data from several radar sites.

Satellite data are from GOES-West, a United States geostationary satellite situated at 105°W during the experiment.

c. Upper-air data

The PRE-STORM upper-air network included the 15 surrounding NWS sounding sites as well as 12 supplemental sites within the PRE-STORM area (Fig. 6). The data were interpolated to 25-mb levels, with the surface kept as an additional level.

The availability of the supplemental soundings was highly variable (Meitín and Cunning 1985). During most of the cases, soundings were taken at least at 3-h intervals and as often as every 90 min. For several cases few, if any, supplemental soundings were taken.

In this paper the upper-air data were used to construct soundings and to derive various stability and thermodynamic parameters: convective inhibition (CIN; Colby 1983), convective available potential energy (CAPE; Moncrieff and Miller 1976; Weisman and Klemp 1982), and bulk Richardson number (Ri; Moncrieff and Green 1972; Weisman and Klemp 1982), which were calculated using the expressions from Bluestein and Jain (1985). For purposes of completeness, several other familiar sounding parameters presented in Houze et al. (1990) were calculated for limited comparison. Comparisons of computed parameters with the studies of Bluestein and Jain (1985) and Houze et al. (1990) should be viewed with caution. Due to the focus of Bluestein and Jain on the near environment of the severe convective line development, the instability may be expected to exceed that found in this study due to our focus on the entire life cycle. The Houze et al. study used standard, twice-daily soundings from only a single site, and near-environment soundings were not always available; hence, somewhat more stable conditions than those of this study may be expected.

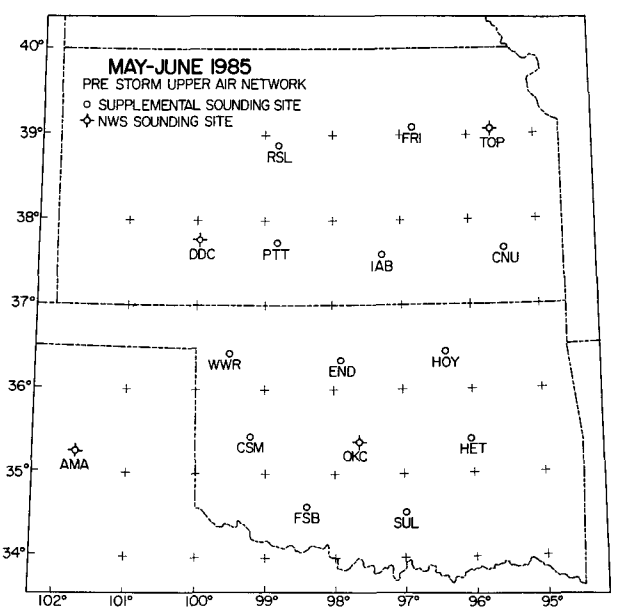

FIG. 6. The PRE-STORM upper-air mesonetwork. Crossed circles indicate NWS sites. Plain circles indicate supplemental sites.

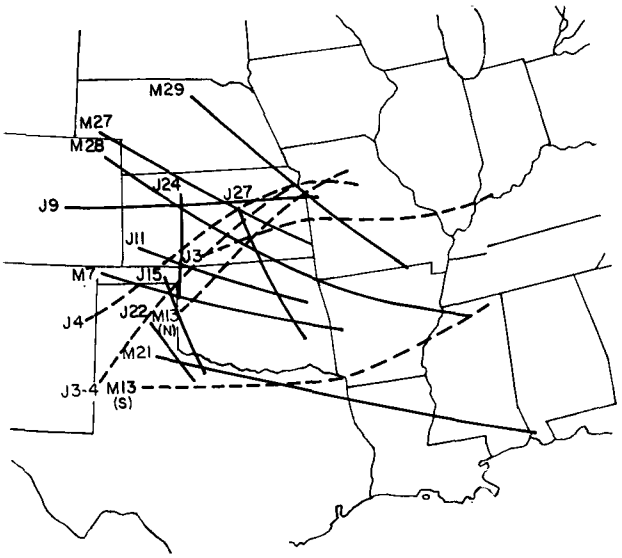

FIG. 7. Tracks (northward-moving systems are dashed; southward-moving systems are solid) of the precipitation and upper cloud centroid of the 16 MCSs examined in the study (M and J refer to May and June, respectively).

3. Case selection

Approximately 25 MCSs traversed at least a portion of the PRE-STORM radar network during May and June (Blanchard 1990). Not all of these systems, however, were adequately sampled by the radar and surface mesonetwork to determine their life cycle characteristics. Since we have found that the wake low is an important indicator of the transition to asymmetric structure, cases were selected that had their wake lows pass through the networks. There were several MCSs that had their convective regions within the mesonet, but their stratiform areas, and hence any wake lows, were outside of the mesonet. This additional requirement led to the loss of several MCSs that developed and moved on the periphery of the surface mesonetwork, leaving a total sample of 16 MCSs. The cases examined for this study included seven that occurred in May and nine in June (Table 1). Also included in Table 1 are the calculated system velocities. Eight of the systems met the MCC criteria (Augustine and Howard 1988) established by Maddox (1980). The tracks of the approximate precipitation and upper cloud centroids for the 16 MCSs are presented in Fig. 7. Such tracks are more difficult to develop than those developed for MCCs (e.g., Maddox 1980) due to the difficulty in locating a true "centroid" given the variety of shapes and sizes of the upper cloud features of these MCSs. Most of the tracks are either from the northwest to southeast or southwest to northeast. Straight north-to-south or west-to-east movement was more rare.

4. Pre-MCS large-scale environment

The basic large-scale environmental conditions found in the PRE-STORM region prior to the development of the MCSs are summarized schematically in Fig. 8. In general, these features are similar to those described by Maddox (1983) in the genesis region of MCCs. There are some cases that differ significantly from the basic schematic and some of these will be discussed.

Many of the cases had a nearly east–west-oriented quasi-stationary front near the Kansas–Oklahoma border. This pattern changed considerably by mid-to-late June as the MCSs at this time were found more often in connection with northeast–southwest-oriented cold fronts extending across northwestern Kansas and moving to the southeast. The nature of this change in frontal structures was not examined. The systems developed and moved in all regions relative to the surface fronts. Relative to the stationary fronts, MCSs developed to the north (e.g., 3–4 June) and to the south (e.g., 13 May southern MCS) in about equal proportions. Two MCSs (27 May and 24 June) developed along drylines. The 27 May MCS was a special case in that it was dissipating as it initially moved into the mesonet and was then regenerated by the interaction of a dryline and the strong gust front associated with the earlier convection (Carbone et al. 1990). The ground-relative surface flow, in relation to the surface fronts, was quite similar among all of the cases. Ahead of the front, to its south and east, there was a 5–10 m s^{-1} south to southeast flow. To the fronts' rear, north and west, the flow was more out of the east to northeast, also at 5–10 m s^{-1}. Thus, there was often a region of moderate convergence in the frontal zone.

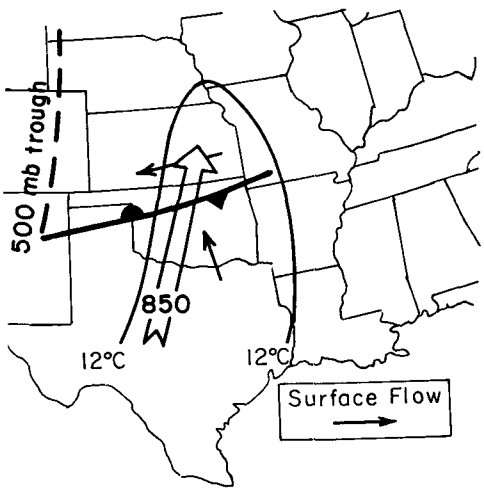

FIG. 8. Schematic of synoptic-scale conditions in the region of MCS development. Dashed line represents the 500-mb short wave. Solid curve is the 12°C, 850-mb dewpoint contour. Small arrows are the surface flow; large arrow is the 850-mb jet.

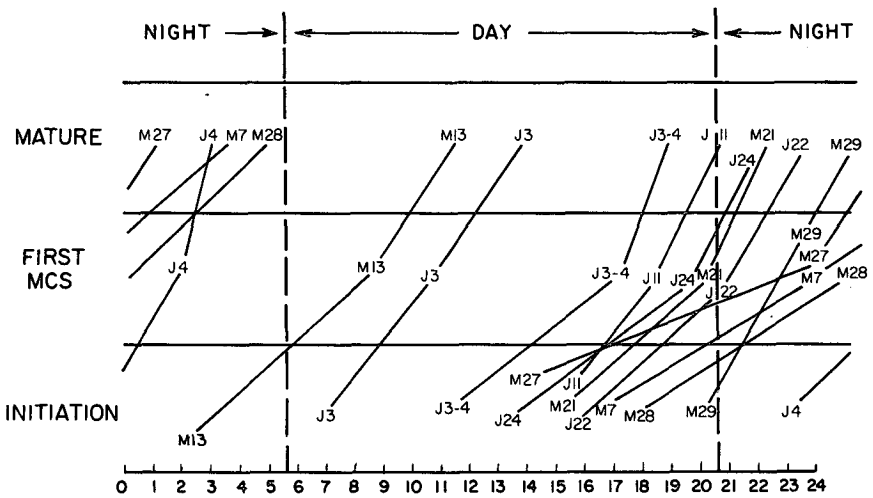

FIG. 9. The diurnal variation of PRE-STORM MCS stages as defined by their radar patterns. See text for an explanation of the terms (M and J refer to May and June, respectively). M13 refers to the southern MCS on 13 May. Abscissa is local standard time.

A low-level jet (LLJ; Bonner 1968) was found to be present in each of the cases at 850 mb, with wind speeds typically about 10–20 m s^{-1} out of the south to southwest. The supplemental soundings showed that as the MCS approached, the LLJ typically strengthened by about 5 m s^{-1}. Such LLJs have been shown to be important precursors of MCS development (Augustine and Caracena 1994). The LLJ was typically found along an axis of moisture-laden air (identified as $T_d \geq 12$°C at 850 mb in Fig. 8) extending from the Texas Gulf coast northward through central and eastern Oklahoma and Kansas. The variation of this moisture-laden air was found to be mainly in its western extent, which depended on the position of the surface fronts and/or drylines.

At 500 mb there was generally a weak short-wave trough extending from extreme western South Dakota through eastern Colorado and eastern New Mexico. However, some cases were found in conjunction with deep troughs (13 May; 3, 3–4, 4, and 26–27 June) and the main trough on 3–4 June was located in the extreme southwestern United States. The PRE-STORM region itself was generally under a weak ridge or on the western edge of a ridge over the southeastern United States.

5. Diurnal variation of MCS stages

While the life cycle characteristics of MCCs have been investigated using satellite data (Maddox 1980, 1983; McAnelly and Cotton 1986; Cotton et al. 1989), similar studies for MCSs as a whole have been lacking due to their wide variety of upper cloud features. Because satellite data cannot define the internal structure of MCSs, radar reflectivity data are used here to define stages in their life cycles. Unfortunately, not all stages of the MCSs were viewed within the high-resolution PRE-STORM radar network. In particular, the initiation and dissipation often occurred outside of the PRE-STORM radar network (see Fig. 7). Therefore, relatively poor resolution National Meteorological Center (NMC) radar summary charts were used to augment the digitized PRE-STORM radar data. It is felt that for the purposes of this discussion, these charts were adequate for the determination of initiation since the exact time of initiation was not needed given the already subjective nature of the remainder of the stages. Unfortunately, the time of MCS dissipation was difficult to ascertain from these NMC charts due to the frequent presence of other convection and difficulties in separating MCS convection from other convective areas. Due to these factors, the dissipating stage is not included in this discussion.

The evolution of three stages in the life cycles of 12 of the 16 MCSs is shown in Fig. 9. The first stage is termed "initiation" and is defined as the time of first convective development. The second stage is termed "first MCS" and is based on the subjective assessment of when there becomes an organized structure to the convection, such as the initial convection developing into a banded or squall line–type structure. Also, at this time there is the initial development of a region of stratiform precipitation (leading or trailing). The third stage, and last examined here, is the "mature" stage, which is defined to be the time when the MCS achieves its greatest degree of organization. This includes the development of a region of enhanced stratiform precipitation as well as a continuing, vigorous line of convection.

It is apparent from Fig. 9 that the majority of the MCSs underwent similar diurnal variations of their stages. The initial cell development typically occurred during the afternoon hours [1100–2000 LST (local

standard time)]. The development of MCS-like precipitation structures usually first became apparent during the evening to early nighttime hours (1700–0000 LST). The mature stage was reached during the overnight hours in most cases (2000–0500 LST). This timing of development is quite similar to that found by Maddox (1980), McAnelly and Cotton (1989), and Cotton et al. (1989) in their studies of MCCs.

This basic cycle of organization occurred in 9 of the 12 MCSs shown in Fig. 9 and 11 of all 16 MCSs examined. Exceptions were on 13 May [southern MCS (see Figs. 7 and 9)], 3 and 4 June (Fig. 9), 13 May [northern MCS (see Fig. 7), not shown], and 27 June (not shown). In these latter cases, strong synoptic forcing mechanisms were present. The 3 and 4 June cases occurred in response to a rather extensive amount of low-level warm advection and frontal lifting that continually destabilized the PRE-STORM region (Trier and Parsons 1993). Both 13 May MCSs, as well as the 27 June MCS, were associated with strong frontal cyclones, strong low-level warm advection, and deep upper-level troughs. The 13 May MCSs developed in areas of generally high instability and CAPE. The 27 June case was strongly forced by a cold front in a tropical-like environment (Trier et al. 1991).

6. MCS surface pressure and precipitation life cycle characteristics

The surface pressure and precipitation features associated with the early stages of the 16 MCSs varied widely. However, as the storms evolved, repeatable patterns tended to appear during the mature-to-dissipating stages. In particular, the maximum pressure gradient associated with the wake low was established during the mature-to-dissipating stage (Williams 1953; Fujita 1955; Pedgley 1962; Johnson and Hamilton 1988; Johnson et al. 1989; Stumpf et al. 1991). This is consistent with the conceptual model of Fujita (1963). In addition, the wake lows were typically found at the northern end of the storms near the back edge of the enhanced stratiform regions (Johnson and Hamilton 1988; Johnson et al. 1989; Stumpf et al. 1991). At least 12 of the 16 MCSs (75%) developed this remarkably similar structure at this time. Eleven of these MCSs are depicted in Fig. 10 at this deep wake-low stage. The 21 May MCS (not shown) also had a similar reflectivity structure as well as a wake low, but the time of its maximum pressure gradient could not be determined since it occurred outside of the mesonet.

At the mature-to-dissipating stages of the 11 MCSs (Fig. 10) the radar reflectivity structure comprised three main features identified in the climatological study of Houze et al. (1990). There was, typically, a leading convective line oriented northeast–southwest. At this late stage the convection was of widely varying intensities, ranging from nearly dissipated (11 June) to intense (28 May). There was often a transition zone behind the convective line having reflectivities generally below 30 dBZ. Also, there was a region of enhanced stratiform precipitation typically found in the left-rear (LR) quadrant of the MCS. The 3, 3–4, and 4 June MCSs, however, also had stratiform precipitation extending into the left-front (LF) quadrant. Typically, the stratiform precipitation region was at or near its maximum extent at this stage. This precipitation structure is very similar to the idealized asymmetric structure defined by Houze et al. (1990), although the enhanced stratiform precipitation region seems to be farther offset (at least for the PRE-STORM year), often being situated well within the LR quadrant, with little, if any, enhanced stratiform precipitation within the other quadrants (except the 3, 3–4, and 4 June cases). Houze et al. do show, however, that there was significant natural variability in the positioning of the enhanced stratiform region.

The surface pressure fields of these MCSs at their mature-to-dissipating stages resembled to some degree those presented by Pedgley (1962). A presquall low, often present earlier, was not visible at this stage as many of the systems had approached the eastern edge of the mesonet. The mesohighs at this stage were expansive features positioned over the convective regions as well as significant portions of the stratiform regions. The wake low was to the rear of the region of enhanced stratiform precipitation and at the back edge of the precipitation in most cases.

The pressure gradients found in these MCSs were often intense and concentrated in two areas. First, there was sometimes a strong leading pressure gradient ahead of the mesohigh associated with the gust front (not visible in Fig. 10). Second, and often the more intense of the two, was the gradient between the mesohigh and wake low. This intense pressure gradient was usually found along the back edge of, and extended into, the region of enhanced stratiform precipitation (Johnson et al. 1989; Stumpf et al. 1991). The station pressure falls commonly far exceeded those that are termed rapid on the synoptic scale (2 mb h^{-1}). The wake low pressure gradient is far more locally concentrated than the pressure drop depicted by Pedgley (1962), which has important implications for the flow field in this region.

In the study of Houze et al. (1990) it is pointed out that while symmetric and asymmetric patterns were identified as extremes at two ends of the spectrum of convective organization, observations showed a continuum of patterns between these two extremes. The present study expands those findings by revealing that this continuum also exists in time. The asymmetric structure does not appear to be a strict type of MCS, but rather, it is a structure that becomes predominant (at least in 75% of the cases studied here) during the mature-to-dissipating stage of the MCS life cycle (Fig. 10). During much of the life cycle, in fact, the MCSs bear little, if any, resemblance to the asymmetric struc-

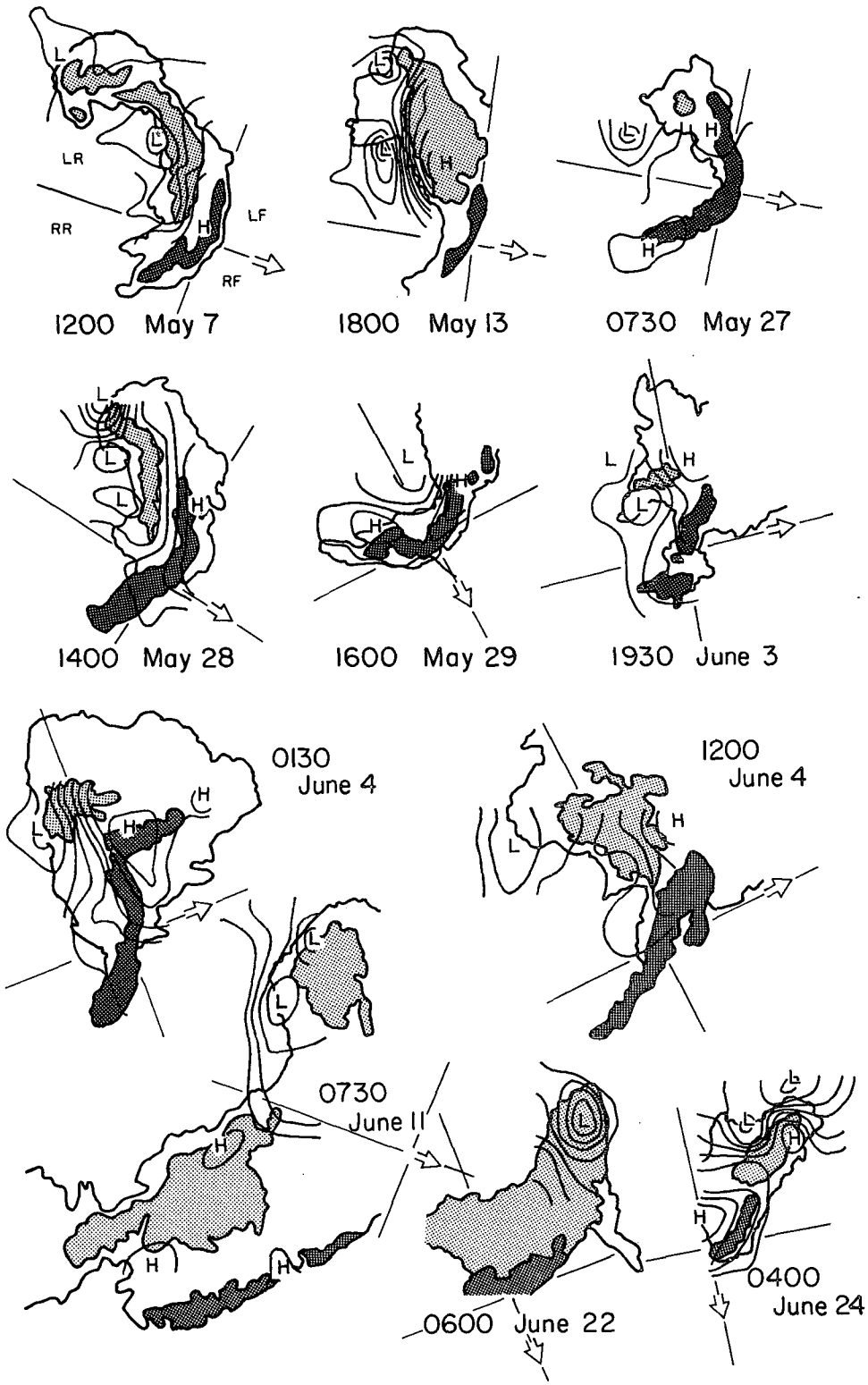

FIG. 10. Plots of MCS structure at time of maximum wake-low pressure gradient. Light shading indicates reflectivities above 30 dBZ (enhanced stratiform). Dark shading represents reflectivities over 40 dBZ (convective line). Outer radar contour is 15 dBZ. Contours are 480-m pressure at 1-mb increments. The 13 May MCS refers to the southern one. Axes along and perpendicular to the storm motion vectors (large arrows) are indicated.

TABLE 2. Maximum wake-low pressure gradients and wake-low and leading edge wind gusts for individual cases. Cases are separated into MCS life cycle classifications (see text). The station of occurrence is in parentheses. Data for 21 May 1985 not available.

Date	Time (UTC)	Maximum wake-low wind gust (m s^{-1}/deg)	Maximum 10-min pressure drop (mb)	Maximum pressure gradient [mb (10 km)$^{-1}$]	Time (UTC)	Maximum leading edge wind gust (m s^{-1}/deg)
Disorganized						
3 June	1920	15.6/74 (P06)	0.9 (P12)	0.5	1925	15.7/349 (P32)
4 June	0940	17.0/119 (P10)	1.9 (P10)	1.0	0930	16.9/343 (P27)
Back building						
27 May	0705	16.5/35 (P05)	1.7 (P05)	1.3	0505	27.1/344 (P11)
28 May	1400	24.6/113 (P06)	6.2 (P06)	3.6	0845	28.9/352 (P10)
29 May	1625	26.5/71 (P08)	3.4 (P08)	2.3	1600	27.6/335 (P08)
Linear						
13 May (southern)	1820	25.9/152 (S21)	6.4 (S17)	5.0	1430	27.3/228 (S29)
11 June	0410	17.0/106 (P28)	3.1 (P19)	2.1	0305	32.3/336 (P41)
22 June	0715	23.3/121 (S02)	1.9 (S02)	2.0	0405	25.5/328 (S02)
24 June	0215	28.8/200 (P03)	2.2 (P10)	2.3	0025	26.5/348 (P10)
Intersecting						
7 May	1230	9.8/112 (S17)	1.1 (S32)	0.8	0845	32.6/324 (S13)
21 May	—	—	—	—	—	—
3–4 June	0205	18.7/104 (P05)	1.8 (P05)	1.6	2310	25.9/311 (S37)

ture. In some cases, they have a symmetric structure during the early stages of development. The prevalence of symmetry early in the life cycle could not be fully examined since many of the MCSs were outside of the PRE-STORM region during that stage.

Four general paths that the MCSs took to the development of the asymmetry have been identified: *disorganized, back-building, linear, and intersecting convective bands.* Placement of MCSs into these categories was done subjectively. Since there was often more than one significant factor in the development of the asymmetry, the groupings are based on the primary characteristic present in the systems' early stages. Some of the cases exhibited combinations of these characteristics and, therefore, the groupings should not be regarded as absolute. Although four paths to asymmetry were identified for MCSs occurring during May and June 1985, the extent to which these results can be generalized to other times and locations is not known. The following subsections give details on these paths through the discussion of one case associated with each path and summaries of pertinent features of the other MCSs in the group. Also, several systems that did not develop asymmetry within the mesonet are discussed.

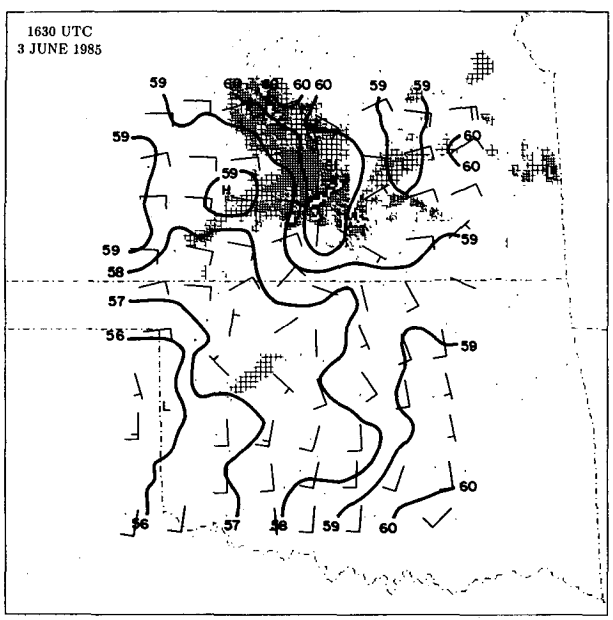

FIG. 11. Pressure at 480 m (mb, leading 9 dropped) at 1630 UTC 3 June 1985. Reflectivity thresholds are 15, 25, 40, and 49 dBZ. Winds are in meters per second, with one full barb equivalent to 5 m s^{-1}.

a. Disorganized

This path to asymmetry was undertaken by only two cases: 3 and 4 June (Table 2).[1] These systems developed under very similar environmental conditions, took similar tracks (Fig. 7), and also had similar developmental cycles. The only major difference between the MCSs was the somewhat larger extent of the 4 June MCS. Both systems developed to the north of a quasi-stationary front that was oriented generally east–west near the Oklahoma–Kansas border (e.g., Fortune et al. 1992; Smull and Augustine 1993; Trier and Parsons 1993; Nachamkin et al. 1994). The MCSs then moved to the northeast into east-central Kansas. The 3 June

[1] Note that the 3 and 4 June cases are distinct from the case labeled 3–4 June.

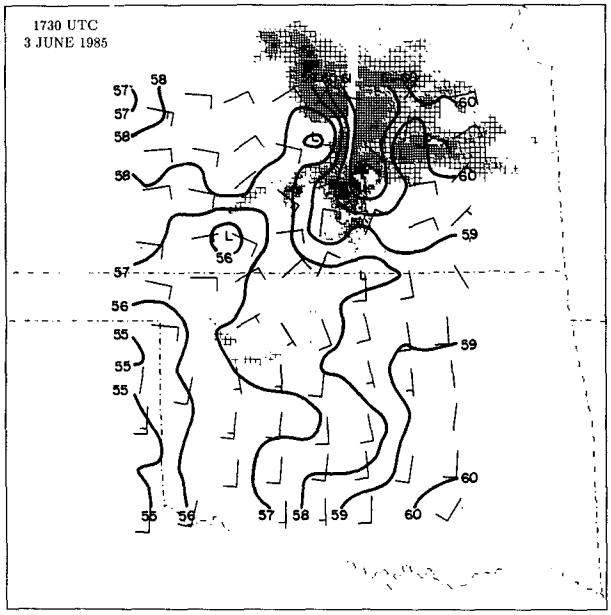

FIG. 12. Same as Fig. 11 except for 1730 UTC 3 June 1985.

MCS is shown here primarily due to its longer presence within the mesonet.

The early stages of these systems (Fig. 11) were characterized by a disorganized convective structure and absence of extensive stratiform precipitation. At this stage, the organization generally resembled the chaotic pattern of Blanchard (1990). The pressure and flow features were generally very weak. Mesolows were found ahead of areas of convection and mesohighs were within convective areas. No wake low was present. The flow was only weakly affected by the MCS at this stage, and there was no organized outflow from the system.

Just 1 h later (Fig. 12), important structural changes had occurred. The northern areas of convection were rapidly dissipating, leaving primarily stratiform precipitation in that region. Convection on the southern flank slightly expanded and intensified. The MCS was beginning to become more organized tending toward the asymmetric pattern that is common in Fig. 10. A presquall mesolow was still present, although it was covered by stratiform precipitation. The mesohigh had strengthened by about 1 mb in 1 h and had expanded to cover much of the stratiform precipitation region. The most significant change was the rapid development of a wake low [also studied by Nachamkin et al. (1994)]. The pressures at the system's rear had decreased by 3 mb in 1 h. An intense gradient developed along the back edge of, and extended into, the stratiform region in a trailing echo notch region (Smull and Houze 1985). A moderate (5.0–7.5 m s^{-1}) northerly outflow developed to the south of the MCS, leading to a small area of convergence that moved along southeastern Kansas into extreme northern Oklahoma. Also, easterly flow in the wake low region strengthened (7.5 m s^{-1}) in response to the increased pressure gradient.

Gradually, the MCS evolved toward an asymmetric pattern (Fig. 13), although it remained more complex than the idealized structure of Houze et al. (1990) throughout its life cycle. The northern portions of the MCS had now become completely stratiform and a region of enhanced stratiform precipitation separated from the convective region. Also, a small northeast–southwest-oriented convective line developed at the southern end of the MCS in response to the outflow-generated convergence. An intense pressure gradient continued within the stratiform region.

Both disorganized MCS cases had generally weak (relative to other MCSs) pressure and flow signatures (Table 2). Sustained winds at the gust front were generally weak to moderate ($\leq$7.5 m s^{-1}) and gusts reached only about 15 m s^{-1} from the northwest, about one-half the strength of the gusts associated with the other systems. The wake low wind gusts for the 3 and 4 June MCSs were generally comparable to the leading edge gusts (15 m s^{-1}) but they had an easterly component. Also, in contrast to the other systems, the maximum wake low and leading edge wind gusts occurred at approximately the same time. The maximum gusts in these disorganized cases occurred around the time of the development of the small convective line and the asymmetry. The maximum wake-low pressure gradient for both cases was below 1 mb (10 km)$^{-1}$ and the maximum 10-min pressure drops were 1–2 mb, both small relative to the other cases, but very large by synoptic-scale standards.

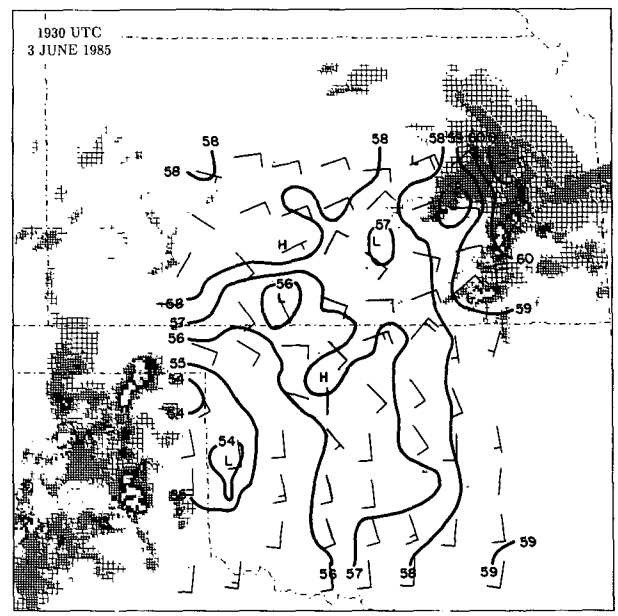

FIG. 13. Same as Fig. 11 except for 1930 UTC 3 June 1985.

These two systems (along with the 3–4 June MCS) were the only PRE-STORM MCSs that developed asymmetry to have significant stratiform precipitation extending into their LF quadrant (see Fig. 10). These 3 cases were also the only ones found in association with strong (20–25 m s^{-1}) mid- and upper-level west-southwest flow due to the presence of a deep upper trough to the west. This flow led to the advection of precipitation particles, in a system-relative sense, to the north (behind) and northeast (ahead) of the convective line. The environmental conditions during the disorganized systems (consisting of just two systems in basically the same synoptic setting) were characterized by strong midlevel southwesterly flow and strong low- and midlevel shear (Table 3). In fact, these systems had the most southerly component to the midlevel flow, due partially to a strong (>20 m s^{-1}) LLJ and a deep upper trough to the west. The instability was moderate with a lifted index (LI) of −6.5°C and a CAPE of 1603 J kg^{-1}. The large shear and moderate CAPE resulted in a fairly low Ri of 32, indicative of the possibility for the development of supercells (Weisman and Klemp 1982), although the severity of these systems was rather limited even in their early stages, due particularly to the highly stable boundary layer conditions found below the frontal surface during these two days. The moisture content of the atmosphere was the highest of any of the groups, with a precipitable water of 4.4 cm, as a result of the strong southerly flow.

In summary, the 3 and 4 June systems were generally very disorganized in their early stages but gradually developed asymmetry very late in their life cycles. The development of the convective line in these cases generally fits into the broken areal category of squall-line development of Bluestein and Jain (1985). The pressure and flow features were relatively weak; even when they were at their deepest point they were far weaker than any of the other asymmetrical MCSs. Other studies have found much stronger pressure gradients in similar frontal overrunning situations (Fujita 1963; Branick et al. 1988) but these were associated with more well developed squall-line systems. Also, the 3 and 4 June MCSs did not develop into the classic asymmetrical structure of Houze et al. (1990) while within the mesonet, possibly due to the lack of the line-end effects, and associated midlevel mesovortex development (Table 1), found in conjunction with more well developed squall-line systems (Skamarock et al. 1994). The existence of strong upper-level shear (Table 3) may have also inhibited mesovortex development (Bartels and Maddox 1991). A mesovortex may have developed in the 4 June MCS, as Fortune et al. (1992) suggested, based on the development of cyclonic vorticity in the stratiform region just prior to the system leaving the PRE-STORM area.

b. Back building

This path to asymmetry was undertaken by the 27, 28, and 29 May MCSs. These MCSs also developed under similar environmental conditions, took similar tracks (Fig. 7), and had similar developmental cycles. All of these systems had their initial development in western Nebraska as a quasi-stationary front extended from along the Colorado Front Range to along the Oklahoma–Kansas border. They then moved to the southeast (Table 1). The 28 May MCS is shown here due to its prolonged presence within the mesonet as well as its intense pressure features.

The early and middle stages of the back-building MCSs were generally characterized by a symmetrical structure. In the 28 May case (Fig. 14), there was a leading northeast–southwest-oriented convective line followed by a region of light stratiform precipitation to

TABLE 3. Mean derived sounding parameters and number of soundings used for the individual categories of MCS life cycle types (see text). Final two columns are from individual nonasymmetrical cases.

	Disorganized	Back building	Linear	Intersecting	15 June	27 June
Vector mean wind 3–10 km [dir (°)/ speed (m s^{-1})]	229/20.7	280/13.6	254/11.3	236/17.0	316/16.7	229/7.4
Vertical shear sfc–6 km [(dir (°)/speed (m s^{-1})]	235/20.0	285/16.2	285/10.8	241/15.0	313/18.3	261/6.8
Lifted index (°C)	−6.5	−6.7	−6.4	−5.8	−5.3	−3.5
Total totals (°C)	54	56	54	55	53	47
K index (°C)	40	29	32	37	31	34
Precipitable water (cm)	4.4	3.0	3.5	3.8	3.6	4.6
Lifted condensation level (mb/km AGL)	837/1.6	798/2.0	799/2.0	836/1.6	782/2.2	836/1.7
Level of free convection (mb/km AGL)	714/3.0	654/3.7	646/3.8	719/2.9	625/4.1	747/2.6
Convective temperature (°C)	29	32	34	29	39	32
Maximum updraft velocity (m s^{-1})	41	48	44	39	42	30
CAPE (J kg^{-1})	1603	1925	1673	1506	1516	1022
CIN (J kg^{-1})	−58	−182	−131	−80	−226	−35
Bulk Ri	32	63	63	38	25	117
Number of soundings	7	13	20	9	6	8

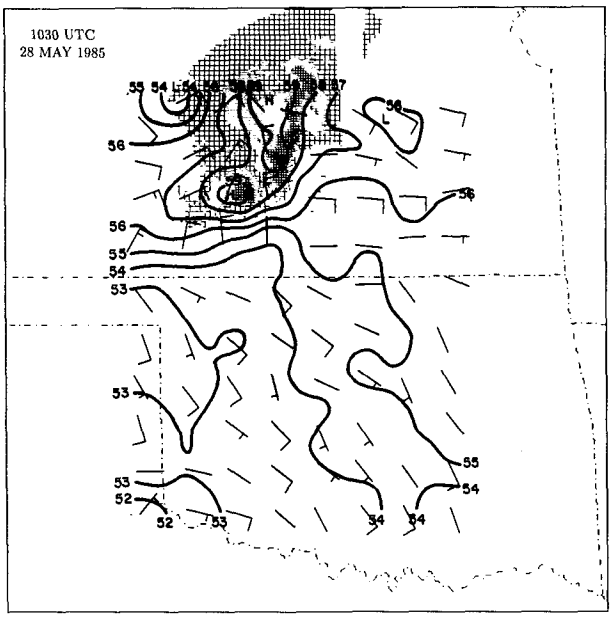

FIG. 14. Same as Fig. 11 except for 1030 UTC 28 May 1985.

the north and west (LR quadrant) of the convective line, leading to an asymmetrical appearance for the MCS. However, the enhanced stratiform precipitation was to the rear of the central portion of the convective line (LR and RR quadrants), and hence its symmetric classification. Moreover, the asymmetric appearance in Fig. 14 may, in part, be due to range effects, that is, a consequence of the radar beam intersecting the upper-level stratiform increasingly at greater distances from the radar (Wichita, Kansas, in this case). Mesohighs were along the convective line and a deep wake low was along the back-central portion of the MCS. An intense pressure gradient was concentrated mostly to the rear of the enhanced stratiform region. Easterly flow exceeding 10 m s^{-1} was strongly accelerating through the wake low. Each MCS on 27, 28, and 29 May had very strong gust fronts with outflows exceeding 25 m s^{-1} from the northwest emanating from the southern portions of the systems and expanding well to their south. These strong outflows led to significant convergence at the southern portions of the MCSs as the northerly outflows met with the generally southeast flow in the environment.

During the remainder of the middle stages (not shown), the northern portions of the convective line began to dissipate as older cells collapsed, leading to the development of a more expansive stratiform area at the northern end of the system. Meanwhile, in the region of enhanced convergence at the southern end of the MCS, convection built back to the southwest. Due to the newness of convection, the southern portions of the MCS were largely lacking in stratiform precipitation. Also, due to the more northeast–southwest orientation of the southern portion of the line, the middle- and upper-level system-relative winds were more along-line and, hence, there was a lack of rearward advection of precipitation particles. These developments in conjunction with a midlevel mesovortex (Houze et al. 1989) led the MCS to take on a highly asymmetric structure by its mature stage (Fig. 15). Concurrently, there was a rapid deepening of the wake low at the back edge of the far northern portion of the stratiform precipitation. A secondary, but weaker, wake low was found along the back edge of the stratiform region to the rear of the northern end of the convective line. The pressure gradient between the mesohigh and northern wake low reached 3.6 mb (10 km)$^{-1}$ with a 6.2-mb drop at PAM station 06 in 10 min (Table 2). The easterly flow through the wake low also strengthened to near severe limits (25 m s^{-1}). The 27 and 29 May cases also had strong winds and intense pressure gradients (Table 2). The 29 May pressure gradient and maximum wind gusts were likely underestimated due to the fact that the central portion of the wake low passed just outside of the mesonet.

This case emphasizes the need to give attention to the wakes of MCSs when forecasting high winds, given that the flow in these regions can be as strong as that associated with the leading gust front. The literature has little information regarding the presence of, and forecasting of, these strong winds in the wake of MCSs. Ely (1982) discussed the significance of the wake of MCSs to the forecasting of gale-force winds in the Gulf of Mexico, but little has been said relative to their possible severity over land. The strong flow in the wakes of the PRE-STORM cases was generally more local-

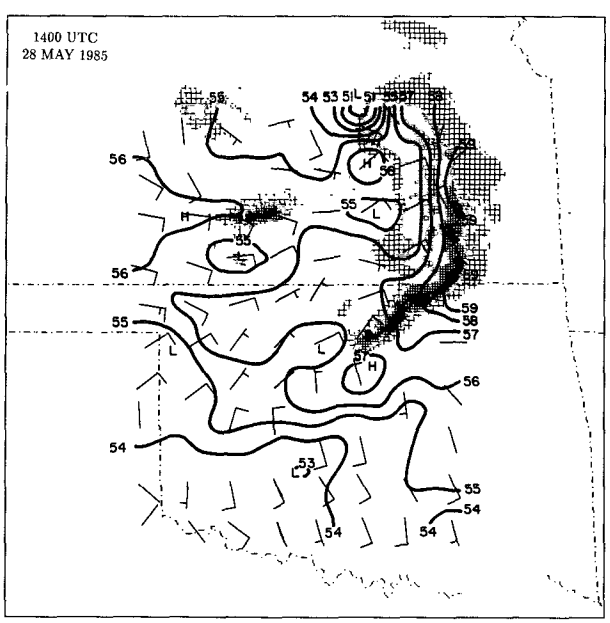

FIG. 15. Same as Fig. 11 except for 1400 UTC 28 May 1985.

ized at the northern end of the MCSs. Also, there was a shift in the location of the strong flow with time. Early in the life cycle of most MCSs (Table 2) the strongest flow was found at the systems' leading edge due to the presence of intense convection and little, if any, wake low. By the mature-to-dissipating stages, the flow was stronger at the rear of the northern portion of the MCSs as the convection had weakened and the wake low strengthened.

Although special soundings were released only for the 27 and 29 May cases, synoptic conditions on 28 May were similar. These systems developed under the influence of moderate west-northwesterly flow at midlevels (Table 3). Also, these systems developed in the most unstable conditions of any of the groups with an LI of −6.7°C and a CAPE of 1925 J kg^{-1}. This result contrasts with the findings of Bluestein and Jain (1985) wherein back-building systems formed under generally more stable conditions than any other classification. The difference may be due to their focus being on the development of the convective line and ours on the entirety of the life cycle. Since back builders, in our classification, were the only of the four groups that continued to develop convection throughout their entire life cycles within the PRE-STORM region, the presence of high instability is not surprising. Other groups included MCSs that were, for at least a portion of the time, dissipating within the PRE-STORM region.

In summary, back-building systems typically began with nearly symmetric structures and had very intense leading gust fronts that led to enhanced convergence at the systems' southern ends. The convective line built back to the southwest in the convergence region as the convection in the northern portion of the MCS dissipated, leading the development of the asymmetrical structure. This pattern of development has the closest resemblence to that obtained in the numerical modeling study of Skamarock et al. (1994). They attribute the southwest building of the convective line to the Coriolis turning of the flow emanating from the surface mesohigh. The enhancement of stratiform precipitation [and a midlevel mesovortex, which could be confirmed only for the 28 May MCS (Table 1)] on the northern end is, in part, attributed to the Coriolis (northward) turning of the ascending, buoyant front-to-rear flow in the leading convective line. The pressure features at the asymmetrical stage were intense with gradients approaching 4 mb (10 km)$^{-1}$ at the systems' far northern ends. Also, the easterly flow through the wake low approached severe limits.

c. Linear

This path to asymmetry was undertaken by the 13 May (southern MCS) and 11, 22, and 24 June MCSs. These systems formed under much more variable environmental conditions than those of the previous two sections. A common feature to all but the 24 June case was that they initially developed along and ahead of a surface cold front, which may have contributed to their linear structure. The linear MCS category is basically a full life cycle extension of the Bluestein and Jain (1985) broken line squall-line formation mechanism. Beyond their initially linear, not necessarily symmetric, structure, these MCSs were quite different from one another as well as being very different from those in the other groups. The 11 June MCS was highly symmetric over nearly its entire life cycle (Johnson and Hamilton 1988; Rutledge et al. 1988) before developing asymmetry. The 22 and 24 June MCSs developed asymmetry quickly and contained mesovortices as well as intense heat bursts. The 13 May southern MCS remained linearly oriented and without significant trailing stratiform precipitation for several hours before attaining an asymmetrical structure. The 13 May MCS is used to illustrate these MCSs due to its extreme surface pressure gradients.

At the early stages of the 13 May MCS (Fig. 16) there was a nearly north–south convective line with a narrow zone of stratiform precipitation. The lack of extensive stratiform precipitation at this time may be, in part, attributed to the relatively weak system-relative flow at upper levels (refer to propagation and vector mean wind speeds in Tables 1 and 3, respectively).

A weak presquall mesolow was present in the northern portion of the MCS, where there was also a mesohigh centered over the most intense convection. Strong (15 m s^{-1}; gusts to 27 m s^{-1}) outflow was also evident in this northern region. A weak wake low was along the back edge of the precipitation at the southern end of the mesonet.

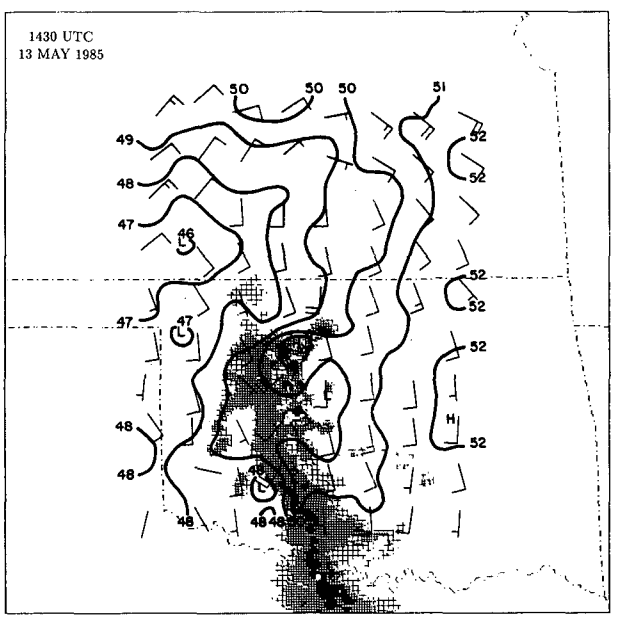

FIG. 16. Same as Fig. 11 except for 1430 UTC 13 May 1985.

By 1700 UTC (not shown) there was a gradual increase in the stratiform precipitation at the system's northern end as the convection in that region gradually dissipated. Concurrently, there was a gradual increase in the pressure gradient in the northern region as the mesohigh strengthened by 2 mb and moved well back into the stratiform region. Also, the wake low deepened by 3 mb at the back edge of the precipitation.

This process continued through 1800 UTC (Fig. 17) as the stratiform precipitation continued to expand and extend well back to the west. The mesohigh continued to strengthen by at least another 1 mb. The wake low had also deepened by another 4 mb and had split into two segments, with one on either side of a westward extension of the stratiform region. This combination of pressure developments led to the formation of the most intense pressure gradient of any of the PRE-STORM cases (Table 2). There was a remarkable 5.0 mb (10 km)$^{-1}$ pressure gradient and a 6.4-mb drop in pressure in a 10-min period, as well as a 4-mb drop in one 5-min period. This intense pressure gradient led to intense, severe-level easterly winds with gusts to 26 m s^{-1}. In fact, there were numerous reports of severe winds in the wake-low region. This MCS nearly fits into the MCS subset of derechos (Johns and Hirt 1987) as it had extensive reports of severe winds extending from southern and eastern Oklahoma into Missouri and Arkansas but did not have the intense wind gusts necessary for inclusion. However, it was different from the documented derechos in that its severe winds were largely confined to the back edge of the MCS rather than at its leading edge. Additionally, the winds had an easterly rather than the westerly component normally associated with squall systems. Unfortunately, special soundings were not available at this stage so the upper-level structure of the system is unknown. The other systems in this group also had intense pressure gradients of around 2 mb (10 km)$^{-1}$. The 22 and 24 June cases also had winds in the wake low approaching or exceeding severe limits. The south-southwest flow through the wake low on 24 June was due to the nearly due north to south movement of the system.

The environmental conditions associated with these systems basically divided into two groups. The 13 May and 11 June MCSs developed under conditions of strong midlevel southwesterly flow as well as strong low- and midlevel shear (Table 3). Also, these two systems had very high instability, similar to the back builders, with an LI of −7°C and CAPEs from 1700 to 2100 J kg^{-1}. In contrast, the 22 and 24 June MCSs developed in weak midlevel westerlies and very little shear. These latter MCSs developed mesovortices, which are known to form in weak flow and weak shear conditions (Bartels and Maddox 1991). The conditions were also slightly more stable with LIs of −5.5°C and CAPEs of 1400 J kg^{-1}.

In summary, MCSs exhibiting initially linear structures were quite variable in their environmental conditions and developmental cycles as compared to the disorganized and back-building MCSs. They ranged from early asymmetrical development (22 and 24 June) to a much more gradual shift to asymmetry from an initially linear MCS (13 May) to a long-lasting highly symmetric structure developing asymmetry at dissipation (11 June). In general, these MCSs are a full life cycle extension of the broken line squall-line formation mechanism of Bluestein and Jain (1985) and are similar to, but more narrowly defined than, the Blanchard (1990) linear MCS structure. The pressure gradients were extremely intense and the easterly flow through the wake low in all but the 11 June MCS approached severe limits.

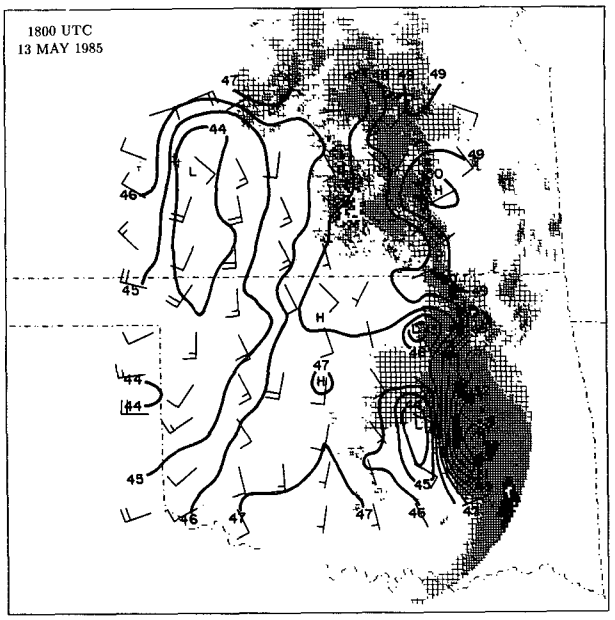

FIG. 17. Same as Fig. 11 except for 1800 UTC 13 May 1985.

d. *Intersecting convective bands*

This path to asymmetry was undertaken by the 7 and 21 May and 3–4 June MCSs. These MCSs, like the linear systems, developed under varying environmental conditions, but they generally developed near an east–west-oriented quasi-stationary front near the Oklahoma–Kansas border region (Brandes 1990). However, the 7 May system moved largely to the south of the front, whereas the 3–4 June MCS moved largely to the north of the front. These MCSs have also been studied by Brandes (1990), Fortune et al. (1992), and Brandes and Zeigler (1993) among others. The 7 May MCS is used to illustrate these MCSs.

At their early stages these systems had the defining characteristic of intersecting bands of convection (Fig. 18). In each case there were two convective bands. The northern convective band was aligned nearly parallel

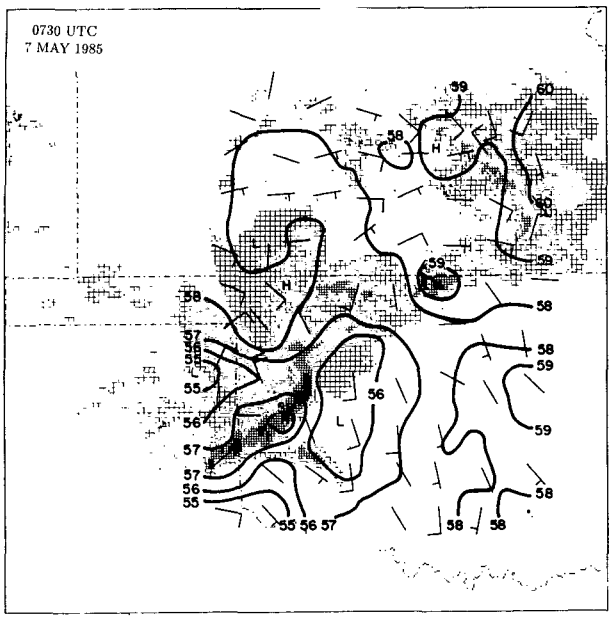

FIG. 18. Same as Fig. 11 except for 0730 UTC 7 May 1985.

to the mean vertical wind shear vector and the southern band extended to the south of the northern band's western end. In general, the northern convective band was considerably weaker and it developed in a region with CAPEs 500–1000 J kg^{-1} less than those found ahead of the southern convective band (Table 3). Similar environmental differences between the bands were also reported by Smull and Augustine (1993) for the 3–4 June MCS. There was also a stratiform region extending to the northwest of the apex of the convective bands. Mesohighs were found along both convective bands. Relatively deep presquall mesolows were found ahead of the southern band. Associated with these features were moderate-to-strong outflows of 15–20 m s^{-1} and gusts in excess of 30 m s^{-1}. Wake lows were found within the precipitation region at the northern end of the MCS as well as a more intense one at the back edge of the enhanced stratiform region associated with the southern band.

During the middle stages (not shown) the northern convective band gradually dissipated leaving behind an expansive area of stratiform precipitation. The southern convective line also weakened somewhat. The trailing stratiform precipitation was also dissipating at its southern end as well as from within. This led to the development of a commalike structure. The wake low was initially at the back edge of the comma head, but it then became a highly transient feature. By the time the comma structure became more fully developed, the mesolow had moved into the heavy precipitation core of the comma head in a region where only 1 h earlier there was a mesohigh. The stratiform precipitation in this region was rapidly dissipating. Brandes and Ziegler (1993) have shown that a strong mesoscale downdraft (15 cm s^{-1} averaged over the entire mesovortex region) was associated with a mesovortex in this trailing stratiform region. However, another mesovortex case, 28 May, showed none of these tendencies for a transient mesolow. The 28 May wake low stayed positioned at the rear of the far northern portion of the system.

Thus, by the late stages (Fig. 19) the MCS had developed a highly asymmetrical commalike structure with an enhanced stratiform region extending well to the north-northwest of the convective line (LR quadrant). Also an intense pressure gradient developed along the back edge of the enhanced stratiform region and a wake low was found at the back edge of the precipitation. In contrast to other MCSs, the wake low with this MCS was not located to the rear of the far northern portion of the MCS, but rather to the rear of the far northern portion of the convective line. It would more closely resemble the other systems if the comma head was not present. By this time, the wake low lost its transient nature as it now stayed positioned along the back edge of the precipitation at the rear of the northern end of the convective line.

The pressure gradients associated with these MCSs were relatively weak [1–2 mb (10 km)$^{-1}$] compared to the linear and back-building systems (Table 2). The 21 May MCS was too far south to get an adequate measure of its pressure gradient. The easterly flow through the wake low on 7 May was very weak (8.5 m s^{-1}). This was probably due to the very short span of the intense gradient in this case. The strong gradient

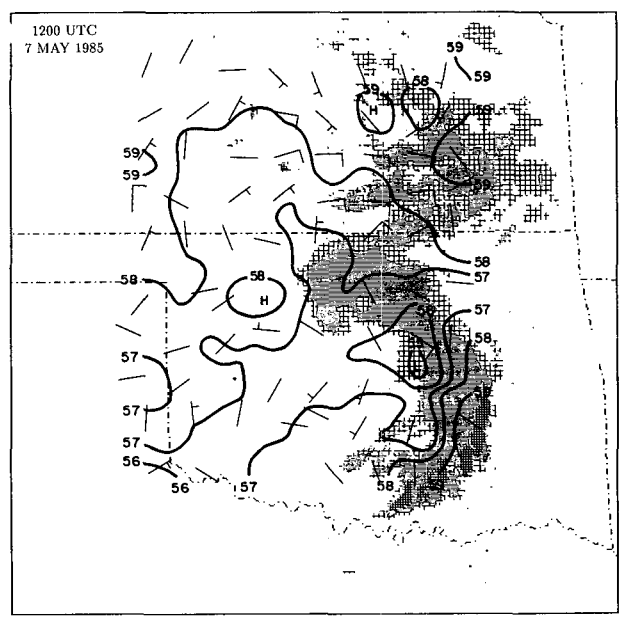

FIG. 19. Same as Fig. 11 except for 1200 UTC 7 May 1985.

lasted for, at most, 15 min as the wake low deepened and decayed with equal rapidity.

The environmental conditions associated with these systems showed significant differences between the mesovortex and nonmesovortex cases, similar to what was found in connection with the linear cases. The 7 and 21 May cases (mesovortex cases) developed under relatively weak midlevel flow (14 m s^{-1}) and moderate instability (LI of −5°C; CAPE of 1153 J kg^{-1}). The 3–4 June MCS, however, developed under strong midlevel flow (19 m s^{-1}) and in a more unstable environment (LI of −7°C; CAPE of 1950 J kg^{-1}), but with highly stable conditions in the boundary layer due to the majority of the system being to the north of the surface front.

In summary, these MCSs were characterized by two intersecting convective bands at their early stages. A northern weak band was aligned nearly parallel to the shear vector and another band extended to its south. This structure has been compared to frontal waves or occlusions (Blanchard 1990; Fortune et al. 1992), but Smull and Augustine (1993) show that such comparisons are inappropriate due to the vastly different processes occurring in the MCSs versus frontal waves. While the MCSs in this group are classified as intersecting bands, it is important to note that they also exhibited back-building characteristics.

e. Nonasymmetric cases

Four cases did not develop an asymmetric structure within the PRE-STORM network. Included in this category are the 13 May (northern MCS) (see Fig. 7) and the 9, 15, and 27 June MCSs. These systems were widely disparate in their development and environment. While these MCSs did not develop asymmetry within the mesonet, they may have done so after exiting the mesonet. The 15 June MCS (discussed momentarily) gave indications of possible asymmetrical development just prior to exiting the mesonet. The 27 June MCS developed and moved directly along a cold front. There was very weak southwest midlevel flow, weak shear, deep moisture, and low-to-moderate instability (Table 3). Since it stayed along the cold front, a more linear-type structure persisted (Trier et al. 1991). However, near the end of its stay within the mesonet a wake low did develop to the rear of its central region and a trend toward asymmetric structure appeared to be occurring as the northern portion of the MCS began to dissipate and the stratiform precipitation region expanded (Lin and Johnson 1994).

The 13 May northern MCS developed in Kansas to the north of the linear 13 May southern MCS in Oklahoma (see Fig. 17). It was to the north of a quasi-stationary front where no soundings were available. It developed a symmetrical structure just prior to exiting the mesonet, and its development afterward was difficult to follow using the NMC summary charts.

The 9 June MCS could never be identified as asymmetrical and it was dissipating as it entered the mesonet. It did, however, have a pronounced mesolow and apparent mesovortex as identified by satellite imagery.

The 15 June system is an example of a system that started to show a tendency for asymmetrical development as it exited the mesonet. The structure of the MCS for most of its life cycle is summarized by that seen at 0430 UTC (Fig. 20). There was a southeastward-moving broken line of convection with a leading stratiform rain region over western Oklahoma. This PRE-STORM MCS was the only one entirely composed of leading stratiform precipitation for any portion of its life cycle. This structure can be explained by examining the system-relative mid- and upper-level flow. The flow at this time throughout Kansas and northern and central Oklahoma was similar to that at Wichita, Kansas (IAB) (Fig. 6), at 0300 UTC. There was a very strong (27 m s^{-1}) northwesterly (295°) vector mean flow at midlevels. From the data in Table 1, a storm-relative flow exceeding 15 m s^{-1} was directed from rear to front, accounting for the existence of leading stratiform precipitation.

Just as the MCS left the mesonet it entered a flow regime more similar to that seen at Cache, Oklahoma (FSB) (Fig. 6), at 0600 UTC. Here, the midlevel flow, while still out of the northwest, was about 20 m s^{-1} weaker than to the north. This change in the environmental flow alone, apart from circulations generated by the storm itself, can explain the development of a system-relative, front-to-rear midlevel flow. The effects of this flow can be seen at 0700 UTC (Fig. 21) as a trail-

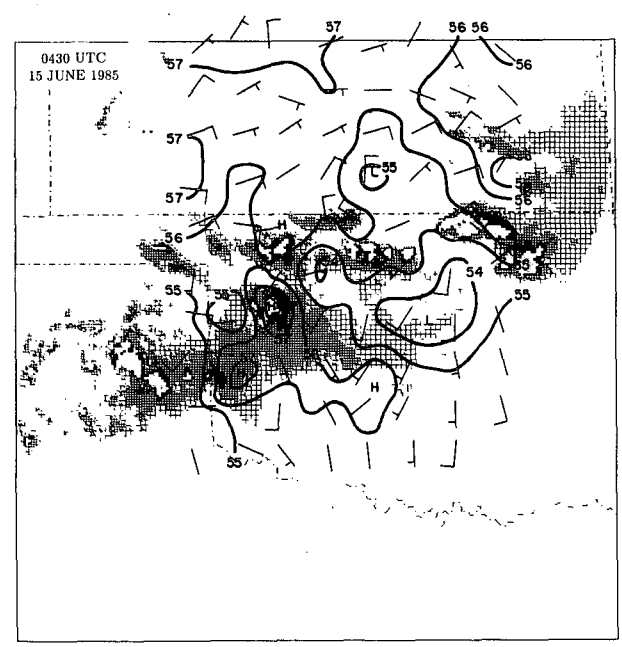

FIG. 20. Same as Fig. 11 except for 0430 UTC 15 June 1985.

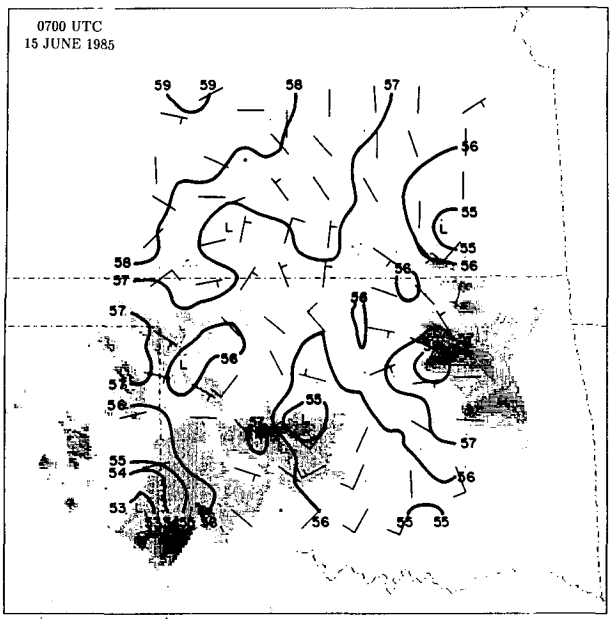

FIG. 21. Same as Fig. 11 except for 0700 UTC 15 June 1985. Reflectivity thresholds are 15, 20, 30, 40, 46, 52, 58, and 61 dBZ.

ing stratiform region had developed. By 0730 UTC (not shown) wake lows had developed at the back edge of the precipitation. But whether this development continued toward an asymmetric pattern is unknown.

7. Synthesis of results and conclusions

Extensive observations from the PRE-STORM field experiment have been used to examine the life cycle characteristics of 16 MCSs that traversed the mesonetwork. The MCSs had large-scale environmental conditions and diurnal variations similar to those found in association with MCCs (e.g., Maddox 1980). Particular attention has been placed on the surface pressure, flow, and precipitation characteristics. It is found that although there was a wide variety of precipitation structures present during the early stages of the MCSs, at least 75% of them developed similar structures during their mature-to-dissipating stages when the wake-low pressure gradient was most intense. At this time, the precipitation structure generally resembled the asymmetric MCS pattern proposed by Houze et al. (1990) and the pressure structure (Fig. 10) was similar to that presented by Pedgley (1962). The symmetric MCS pattern was seen in many of these systems; however, it was typically confined to the earlier stages in the developmental cycle. Therefore, the classifications symmetric and asymmetric refer to the structure at a stage in the life cycle of an MCS rather than a type of MCS. There appears to be a continuum of precipitation patterns, from early stages exhibiting a variety of structures (which in some instances may be symmetric) to later stages, which can be best described as asymmetric (following Houze et al. 1990).

The corresponding surface pressure and ground-relative flow associated with these two patterns are presented in Fig. 22. The reflectivity structure is adapted from Houze et al. (1990). The surface pressure pattern (Fig. 22a) closely follows that presented by Johnson and Hamilton (1988) for the 11 June case. There is a presquall mesolow, mesohigh, and wake low. The mesohigh is centered toward the rear of the convective line at this stage. The wake low is along the back-central portion of the MCS. There is a moderate-to-strong gust front and a moderate wake-low pressure gradient. The flow at this stage is typically strongest (>25 m s^{-1}) at the leading edge of the system and is directed from the northwest (Table 2).

The asymmetric MCS structure (Fig. 22b) bears some resemblance to that presented by Pedgley (1962) and Houze et al. (1990), but the stratiform rain region is displaced farther into the LR quadrant of the MCS. Also, there were three cases that had significant stratiform precipitation in their LF quadrant. This structure characterizes the PRE-STORM MCS cases, but the extent to which it can be generalized to other times and locations is not known. The convective line is generally somewhat weaker at this stage, having the strongest cells on the southern end, and the stratiform precipitation is at or near its maximum extent. There is typically a weaker presquall mesolow at this stage. The mesohigh by this stage has extended well back into the stratiform rain region, which helps to increase the pressure gradient between the mesohigh and the wake low. The gradients become very strong, typically 2 mb (10 km)$^{-1}$ but can be as strong as 5 mb (10 km)$^{-1}$. Very strong flow passes through the wake low, often approaching or exceeding the NWS severe limits (25 m s^{-1}). In contrast to the earlier stages, the strongest surface flow (typically at least 20 m s^{-1}) now has an easterly component and is at the system's rear. This strong flow is usually localized within the wake low region at the northern end of the system. This wake region of squall lines has not received much attention in the literature given the often severe (4 of 11 asymmetric systems had gusts greater than 25 m s^{-1}) nature of the surface flow there.

The recent modeling work of Skamarock et al. (1994) has shown that initially symmetric north–south convective lines will evolve into asymmetric lines in the presence of the Coriolis force. A prominent factor in the enhancement of precipitation on the northern end of the storm was found to be the Coriolis (northward) turning of the ascending, buoyant front-to-rear flow in the leading convective line. In addition, the frequent occurrence of a south-to-north-directed along-line flow at upper levels will tend to transport hydrometeors aloft toward the north end of the line, thereby contributing to an asymmetric stratiform cloud pattern (e.g., Newton and Fankhauser 1964).

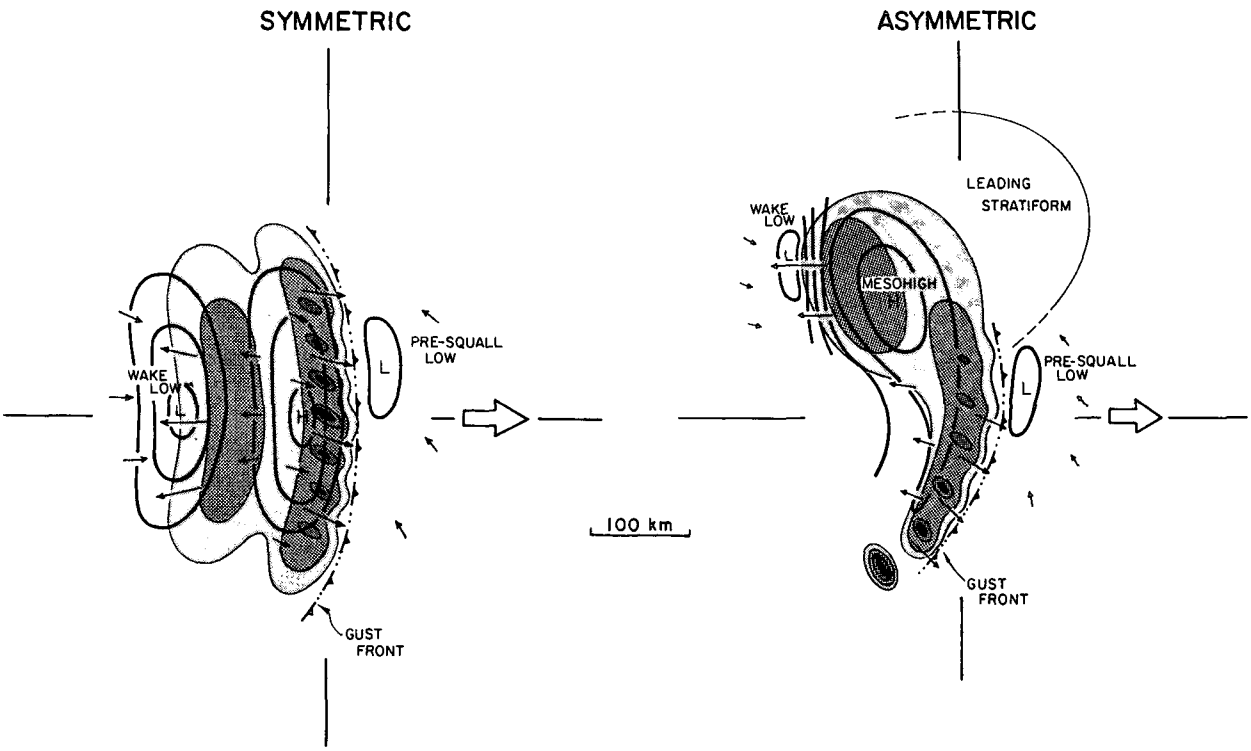

FIG. 22. Conceptual model of the surface pressure, flow, and precipitation fields associated with the (a) symmetric and (b) asymmetric stages of the MCS life cycle. Radar reflectivity field is adapted from Houze et al. (1990). Levels of shading denote increasing radar reflectivity, with darkest shading corresponding to convective cell cores. Pressure is in 1-mb increments. Small arrows represent the surface flow. Lengths of the arrows are proportional to the wind speed found at their center. The large arrows represent the storm motion with quadrants defined in Fig. 1 and text indicated.

A large number of the cases (for which data are available) contained an accompanying midlevel mesovortex within the stratiform region. Numerical simulations by Skamarock et al. (1994) show similar mesovortex development at the northern end of squall lines in association with the evolution of squall lines into asymmetric precipitation structures. Their simulations, however, do not show the strong surface wake lows observed here. The numerical results of Zhang and Gao (1989) suggest that inclusion of the ice phase, omitted in the Skamarock et al. model, is important in obtaining realistic simulations of wake lows. Another point to be made is that while there often appears to be a relationship between the formation of a midlevel mesovortex and asymmetry, there does not appear to be, in most cases, a direct relationship between the midlevel mesovortex and the wake low.

Four apparent paths toward asymmetry were identified from the limited PRE-STORM dataset. They are termed disorganized (two cases), back-building (three cases), linear (four cases), and intersecting convective bands (three cases). Also, four systems did not develop asymmetry while in the PRE-STORM region. Each of these latter MCSs possessed characteristics that delayed or completely prevented the asymmetric development.

The limited number of cases, lack of a clear separation at times between them, and incomplete sounding coverage make it impossible to unambiguously define path types and discriminate between them based on environmental conditions. Moreover, systems classified in the same groupings often exhibited significant differences (e.g., linear and intersecting bands). Clearly, many more cases are necessary to achieve a fully representative dataset.

A major question that remains is whether the tendency of MCSs to develop into an asymmetric pattern later in their life cycles is a general behavior or whether PRE-STORM was an anomalous year. The recent modeling studies of Weisman (1993) and Skamarock et al. (1994) suggest that this behavior may indeed be common. A valuable dataset that may lead to the development of an answer, observationally, is the national-scale, high-resolution NWS WSR-88D radar composites of all United States radars. Such a dataset allows an examination of all MCSs in all regions and over their entire life cycle. Also, the recent addition of numerous automated surface stations and their more frequent observations may allow for adequately detailed pressure observations without executing a costly field project. These relatively new developments in observational systems may lead to

the establishment of a thorough detailed MCS climatology that is long overdue.

Acknowledgments. The authors wish to thank José Meitín, Robert Hueftle, and Diana Bartels at NOAA/NSSL in Boulder, Colorado, for their help in supplying much of the data required for this study. The authors also greatly appreciate the many helpful comments and improvements offered by Robert Maddox, Brad Smull, and an anonymous reviewer. NCAR provided much of the computer time. Judy Sorbie-Dunn drafted several of the figures. The research was supported by the National Oceanic and Atmospheric Administration through the Cooperative Institute for Research in the Atmosphere under Grant NOAA 90 RAH 00077-9-01 and the National Science Foundation under Grants ATM-9013112 and ATM-9313716.

REFERENCES

Augustine, J. A., and K. W. Howard, 1988: Mesoscale convective complexes over the United States during 1985. *Mon. Wea. Rev.*, **116,** 685–701.

——, and F. Caracena, 1994: Lower-tropospheric precursors to nocturnal MCS development over the central United States. *Wea. Forecasting,* **9,** 116–135.

Barnes, S. L., 1964: A technique for maximizing details in numerical weather map analysis. *J. Appl. Meteor.*, **3,** 396–409.

——, 1973: Mesoscale objective map analysis using weighted time-series observations. NOAA Tech. Memo. ERL NSSL-62, Norman, OK, 60 pp.

Bartels, D. L., and R. A. Maddox, 1991: Midlevel cyclonic vortices generated by mesoscale convective systems. *Mon. Wea. Rev.*, **119,** 104–118.

Blanchard, D. O., 1990: Mesoscale convective patterns of the southern High Plains. *Bull. Amer. Meteor. Soc.*, **71,** 994–1005.

Bluestein, H. B., and M. H. Jain, 1985: Formation of mesoscale lines of precipitation: Severe squall lines in Oklahoma during the spring. *J. Atmos. Sci.*, **42,** 1711–1732.

——, G. T. Marx, and M. H. Jain, 1987: Formation of mesoscale lines of precipitation: Nonsevere squall lines in Oklahoma during the spring. *Mon. Wea. Rev.*, **115,** 2719–2727.

Bonner, W. D., 1968: Climatology for the low level jet. *Mon. Wea. Rev.*, **96,** 833–850.

Brandes, E. A., 1990: Evolution and structure of the 6–7 May 1985 mesoscale convective system and associated vortex. *Mon. Wea. Rev.*, **118,** 109–127.

——, and C. L. Ziegler, 1993: Mesoscale downdraft influences on vertical vorticity in a mature mesoscale convective system. *Mon. Wea. Rev.*, **121,** 1337–1353.

Branick, M. L., F. Vitale, C.-C. Lai, and L. F. Bosart, 1988: The synoptic and subsynoptic structure of a long-lived severe convective system. *Mon. Wea. Rev.*, **116,** 1335–1370.

Carbone, R. E., J. W. Conway, N. A. Crook, and M. W. Moncrieff, 1990: The generation and propagation of a nocturnal squall line. Part I: Observations and implications for mesoscale predictability. *Mon. Wea. Rev.*, **118,** 26–49.

Chong, M., P. Amayenc, G. Scialom, and J. Testud, 1987: A tropical squall line observed during the COPT 81 experiment in West Africa. Part I: Kinematic structure inferred from dual-Doppler radar data. *Mon. Wea. Rev.*, **115,** 670–694.

Colby, F. P., Jr., 1983: Convective inhibition as a predictor of the outbreak of convection in AVE-SESAME II. Preprints, *13th Conf. on Severe Local Storms,* Tulsa, OK, Amer. Meteor. Soc., 324–327.

Cotton, W. R., M. S. Lin, R. L. McAnelly, and C. J. Tremback, 1989: A composite model of mesoscale convective complexes. *Mon. Wea. Rev.*, **117,** 765–783.

Cunning, J. B., 1986: The Oklahoma–Kansas preliminary regional experiment for STORM-Central. *Bull. Amer. Meteor. Soc.*, **67,** 1478–1486.

Doswell, C. A. III, 1991: Comments on mesoscale convective patterns of the southern high plains. *Bull. Amer. Meteor. Soc.*, **72,** 389–390.

Ely, G. F., 1982: Case study of a significant thunderstorm wake depression along the Texas coast: May 29–30, 1981. NOAA Tech. Memo. NWS SR-105, National Weather Service, 64 pp.

Fortune, M. A., W. R. Cotton, and R. L. McAnelly, 1992: Frontal wave–like evolution in some mesoscale convective complexes. *Mon. Wea. Rev.*, **120,** 1279–1300.

Fujita, T. T., 1955: Results of detailed synoptic studies of squall lines. *Tellus,* **7,** 405–436.

——, 1959: Precipitation and cold air production in mesoscale thunderstorm systems. *J. Meteor.*, **16,** 454–466.

——, 1963: Analytical mesometeorology. A review. *Meteor. Monogr.*, **5,** 77–125.

——, 1978: Manual of downburst identification for project NIMROD. Satellite and Mesometeorology Res. Pap. No. 156, University of Chicago, Dept. of Geophysical Sciences, 104 pp.

Garratt, J. R., and W. L. Physick, 1983: Low-level wind response to mesoscale pressure systems. *Bound.-Layer Meteor.*, **27,** 69–87.

Houze, R. A., Jr., S. A. Rutledge, M. I. Biggerstaff, and B. F. Smull, 1989: Interpretation of Doppler weather radar displays of midlatitude mesoscale convective systems. *Bull. Amer. Meteor. Soc.*, **70,** 608–619.

——, B. F. Smull, and P. Dodge, 1990: Mesoscale organization of springtime rainstorms in Oklahoma. *Mon. Wea. Rev.*, **118,** 613–654.

Hoxit, L. R., C. F. Chappell, and J. M. Fritsch, 1976: Formation of mesolows or pressure troughs in advance of cumulonimbus clouds. *Mon. Wea. Rev.*, **104,** 1419–1428.

Johns, R. H., and W. D. Hirt, 1987: Derechos: Widespread convectively induced windstorms. *Wea. Forecasting,* **2,** 32–49.

——, K. W. Howard, and R. A. Maddox, 1990: Conditions associated with long-lived derechos—An examination of the large-scale environment. Preprints, *16th Conf. on Severe Local Storms,* Kananaskis Park, Alberta, Canada, Amer. Meteor. Soc., 408–412.

Johnson, R. H., and J. J. Toth, 1986: Preliminary data quality analysis for May–June 1985 Oklahoma–Kansas PRE-STORM PAM-II mesonetwork. Atmospheric Science Paper No. 407, Colorado State University, Dept. of Atmospheric Science, Fort Collins, CO, 41 pp.

——, and P. J. Hamilton, 1988: The relationship of surface pressure features to the precipitation and airflow structure of an intense midlatitude squall line. *Mon. Wea. Rev.*, **116,** 1444–1472.

——, S. Chen, and J. J. Toth, 1989: Circulations associated with a mature-to-decaying midlatitude mesoscale convective system. Part I: Surface features—Heat bursts and mesolow development. *Mon. Wea. Rev.*, **117,** 942–959.

Kane, R. J., C. R. Chelius, and J. M. Fritsch, 1987: Precipitation characteristics of mesoscale convective weather systems. *J. Climate Appl. Meteor.*, **26,** 1345–1357.

Lin, X., and R. H. Johnson, 1994: Heat and moisture budgets and circulation characteristics of a frontal squall line. *J. Atmos. Sci.*, **51,** 1661–1681.

Loehrer, S. M., 1992: The surface pressure features and precipitation structure of PRE-STORM mesoscale convective systems. Atmospheric Science Paper No. 518, Colorado State University, Dept. of Atmospheric Science, Fort Collins, CO, 296 pp.

Maddox, R. A., 1980: Mesoscale convective complexes. *Bull. Amer. Meteor. Soc.*, **61,** 1374–1400.

——, 1983: Large-scale meteorological conditions associated with midlatitude, mesoscale convective complexes. *Mon. Wea. Rev.*, **111,** 1475–1493.

McAnelly, R. L., and W. R. Cotton, 1986: Meso-β-scale characteristics of an episode of meso-α-scale convective complexes. *Mon. Wea. Rev.*, **114,** 1740–1770.

——, and ——, 1989: The precipitation life cycle of mesoscale convective complexes over the central United States. *Mon. Wea. Rev.*, **117,** 784–808.

Meitín, J. G., and J. B. Cunning, 1985: The Oklahoma–Kansas preliminary regional experiment for STORM-Central (OK PRESTORM), Volume I. Daily operations summary. NOAA Tech. Memo. ERL ESG-20, Dept. of Commerce, Weather Research Program, Boulder, CO, 313 pp.

Moncrieff, M. W., and J. S. A. Green, 1972: The propagation and transfer properties of steady convective overturning in shear. *Quart. J. Roy. Meteor. Soc.*, **98,** 336–352.

——, and M. J. Miller, 1976: The dynamics and simulation of tropical cumulonimbus and squall lines. *Quart. J. Roy. Meteor. Soc.*, **102,** 373–394.

Nachamkin, J. E., R. L. McAnelly, and W. R. Cotton, 1994: An observational analysis of a developing mesoscale convective complex. *Mon. Wea. Rev.*, **122,** 1168–1188.

Newton, C. W., and J. C. Fankhauser, 1964: On the movements of convective storms, with emphasis on size discrimination in relation to water-budget requirements. *J. Appl. Meteor.*, **3,** 651–688.

Pedgley, D. E., 1962: A meso-synoptic analysis of the thunderstorms on 28 August 1958. Memo. No. 106, British Meteorological Office, Geophysics, 74 pp.

Rutledge, S. A., R. A. Houze, Jr., M. I. Biggerstaff, and T. Matejka, 1988: The Oklahoma–Kansas mesoscale convective system of 10–11 June 1985: Precipitation structure and single-Doppler radar analysis. *Mon. Wea. Rev.*, **116,** 1409–1430.

Skamarock, W. C., M. L. Weisman, and J. B. Klemp, 1994: Three-dimensional evolution of simulated long-lived squall lines. *J. Atmos. Sci.*, **51,** 2563–2584.

Smull, B. F., and R. A. Houze Jr., 1985: A midlatitude squall line with a trailing region of stratiform rain: Radar and satellite observations. *Mon. Wea. Rev.*, **113,** 117–133.

——, and ——, 1987: Dual-Doppler radar analysis of a midlatitude squall line with a trailing region of stratiform rain. *J. Atmos. Sci.*, **44,** 2128–2148.

——, and J. A. Augustine, 1993: Multiscale analysis of a mature mesoscale convective complex. *Mon. Wea. Rev.*, **121,** 103–132.

Stumpf, G. J., R. H. Johnson, and B. F. Smull, 1991: The wake low in a midlatitude mesoscale convective system having complex organization. *Mon. Wea. Rev.*, **119,** 134–158.

Trier, S. B., and D. B. Parsons, 1993: Evolution and environmental conditions preceding the development of a nocturnal mesoscale convective complex. *Mon. Wea. Rev.*, **121,** 1078–1098.

——, ——, and J. H. E. Clark, 1991: Environmental and evolution of a cold-frontal mesoscale convective system. *Mon. Wea. Rev.*, **119,** 2429–2455.

Vescio, M. D., and R. H. Johnson, 1992: The surface-wind response to transient mesoscale pressure fields associated with squall lines. *Mon. Wea. Rev.*, **120,** 1837–1850.

Weisman, M. L., 1993: The genesis of severe, long-lived bow echoes. *J. Atmos. Sci.*, **50,** 645–670.

——, and J. B. Klemp, 1982: The dependence of numerically simulated convective storms on vertical wind shear and buoyancy. *Mon. Wea. Rev.*, **110,** 504–520.

Williams, D. T., 1953: Pressure wave observations in the central Midwest, 1952. *Mon. Wea. Rev.*, **81,** 278–298.

——, 1954: A surface study of a depression-type pressure wave. *Mon. Wea. Rev.*, **82,** 289–295.

Zhang, D.-L., and K. Gao, 1989: Numerical simulation of an intense squall line during 10–11 June 1985 PRE-STORM. Part II: Rear inflow, surface pressure perturbations and stratiform precipitation. *Mon. Wea. Rev.*, **117,** 2067–2094.

Zipser, E. J., 1977: Mesoscale and convective-scale downdrafts as distinct components of squall-line structure. *Mon. Wea. Rev.*, **105,** 1568–1589.